



A review of retinal blood vessels extraction techniques: challenges, taxonomy, and future trends

Khan Bahadar Khan^{1,2,4}  · Amir A. Khaliq² · Abdul Jalil² · Muhammad Aksam Iftikhar³ · Najeeb Ullah⁴ · Muhammad Waqar Aziz⁴ · Kifayat Ullah⁴ · Muhammad Shahid⁵

Received: 27 July 2017 / Accepted: 25 September 2018
© Springer-Verlag London Ltd., part of Springer Nature 2018

Abstract

The visual exploration of retinal blood vessels assists ophthalmologists in the diagnoses of different abnormalities of the eyes such as diabetic retinopathy, glaucoma, cardiovascular ailment, high blood pressure, arteriosclerosis, and age-related macular degeneration. The manual inspection of retinal vasculature is an extremely challenging and tedious task for medical experts due to the complex structure of an eye, tiny blood vessels, and variation in vessels width. Several automatic retinal vessels extraction techniques have been proposed in contemporary literature, which assist ophthalmologists in the timely identification of an eye disorders. However, due to the fast evolution of such techniques, a comprehensive survey is needed. This survey presents a comprehensive review of such techniques, strategies, and algorithms presented to date. The techniques are classified into logical groups based on the underlying methodology employed for retinal vessel extraction. The performance of existing techniques is reported on the publicly accessible datasets in term of various performance measures, providing a valuable comparison among the techniques. Thus, this survey presents a valuable resource for researchers working toward automatic extraction of retinal vessels.

Keywords Vessels segmentation · DRIVE · STARE · Retina images · Survey · Review

1 Introduction

The human fundus RGB photographs are the projection of the inner surface of an eye. Retinal images are widely used in a noninvasive way by medical experts in the analysis of visual impairments [1]. In the early 1960s, optical photography made an important contribution in the medical prescription [2]. The first photographic retina images

indicating blood vessels were discovered by German ophthalmologist, Gerloff in 1891. Gullstrand first developed the fundus camera in 1910 [3]. Herbert and Michael expressed that the advancement of ocular photographs and expanding research in fundus photograph examination may be because of the necessities of clinical procedure to discover better and less expensive methods of diagnosing, classifying, and screening fundus abnormalities [4].

The fundus image of the retina uncovers its structural format such as retinal vessels map, optic disk (OD), fovea, macula, and pathological structures such as microaneurysms (MAs), hemorrhages, exudates, cotton wool spots, if exist [5]. The optic nerve head begins from OD (observed as a bright oval shape) and is the passage point for major vessels to the eye. Macula (exposed as a dull zone without vessels) with the fovea at its middle is responsible for central and high-resolution eyesight. The blood vessel network has a high contrast due to high frequency stretched over the entire fundus image. The retinal veins provide blood supply to the retina and transmit the data signals from the retina to the brain [6].

✉ Khan Bahadar Khan
kb.khattak@gmail.com

¹ Department of Telecommunication Engineering, University College of Engineering and Technology (UCET), The Islamia University, Bahawalpur, Pakistan

² Department of Electrical Engineering, International Islamic University, Islamabad, Pakistan

³ Department of Computer Science, Comsats Institute of Information Technology, Lahore, Pakistan

⁴ Department of Computer Science, CECOS University, Peshawar, KPK, Pakistan

⁵ PAVIS - Pattern Analysis and Computer Vision Lab, The Istituto Italiano di Tecnologia - IIT, Genoa, Italy

Retinal vessel extraction and characterization of morphological attributes such as diameter, shape, tortuosity, and bifurcation can be utilized in screening, evaluation, and medication purposes of different eye abnormalities [7]. The retinal vasculature variation is used as an indication for detection of different abnormalities such as DR, hypertensive retinopathy, retinal artery/vein occlusion, and other disorders, for example stroke, hypertension and diabetes, induced modifications in the structure of retinal vessels. Evaluation of retinal blood vessel attributes, for example variation in width, is utilized to analyze hypertension, while bifurcation points and tortuosity can help with the identification of cardiovascular ailments and DR [8]. Most of the retinal diseases that produce alterations in the retinal vessel structure would cause visual impairments. Eyesight can be prevented largely by the detection of such pathologies at the initial stage [9].

Automatic precise identification and diagnoses of eye abnormalities and their timely medication are important in restraining blindness. However, any computerized examination of the retinal vessel structure needs its accurate extraction first. Traditionally, manual segmentation is performed by trained experts that is very hard and time-consuming task [10]. Moreover, the complexities in the imaging procedure, such as the lower contrast difference between vessel and non-vessel pixels, unbalanced background illumination and the vessel width variation, brightness and shape, reduce significantly the coincidence among segmentations performed by various human graders [11]. These facts stimulate the advancement of automatic techniques for retinal vessel extraction without human interference.

Various retinal vessel segmentation techniques in the literature are summarized in different survey and reviews. For example, Mabrouk et al. [12] introduced a concise review of retinal detection and registration techniques, which restrict explanation to the detection of the centers and boundaries of retinal vessels. John et al. [13] and Oliver et al. [14] discussed different frameworks for screening of DR in fundus images. Fraz et al. [6] presented an extensive review of the different methods and algorithms for extraction of retinal vessels. They provide a comprehensive study of various retinal vessel detection algorithms; pros and cons of different techniques; current patterns and future guidelines and outline the open issues. They discussed a limited number of retinal image datasets. The most recent survey discusses the techniques for retinal vessel detection and challenges associated with retina evaluation [7].

In this article, we have discussed the retinal image acquisition and different abnormalities associated with it. Comparison tables of all openly accessible datasets are added. The target of this article is to inspect various retinal vessel detection schemes; to show a comparison of different techniques utilized for retinal vessel extraction; to disclose the

pros and cons of various methods; to discuss future guidelines and outline the open issues. We have covered a wide range of published papers from the beginning until now and also divide these articles into different logical categories based on the image processing techniques to make it easier for readers. All the retinal datasets developed until now are also summarized in this paper.

The following are the major contributions:

- Table 1 is added for comparison of all openly accessible retinal image datasets. In the literature, Fraz et al. [6] discussed only eight (8) datasets, while this article has compared thirteen (13) openly accessible datasets.
- We have classified the retinal vessels segmentation approaches into more logical groups than Fraz et al. [6] for the ease of readers.
- Fraz et al. [6] selected and compared only 69 papers from peer-reviewed publications, while we have compared and evaluated 149 papers from the peer-reviewed journals.
- In the 4th column of Table 3, we have summarized results for medical examination and applications.
- In Sect. 4, we have added Fig. 6 to show frequency of databases, which is frequently used for validation of different retinal vessel extraction algorithms.

This article consists of the following sections: retinal image analysis (Sect. 2), published literature that investigated retinal vessels extraction techniques (Sect. 3), and discussion and the conclusion (Sect. 4).

2 Retinal image analysis

This section discusses the acquisition and abnormalities of retinal images and the datasets used for validation of retinal vessels extraction techniques.

2.1 Acquisition of retinal image

Retinal photographs are captured by a digital fundus camera attached with a low-power microscope. Pupil of the human eye is used as entry/exit points for fundus camera illumination and imaging light beams on the inner surface of the eye called the retina. Visible landmarks of the retina are OD, blood vessels, macula, and fovea. The fundus camera operates in different modes to scrutinize the human eye retina. In color mode, the retina is inspected in full color under the flashing of white light. In red-free mode, a filter is applied to improve the appearance of vessel network to observe vascular disorders within the retina. It is used to examine disorders such as hemorrhages, exudates, nerve fiber layer defects, and epiretinal membranes. In angiography mode, fluorescent dye is vaccinated into the blood

Table 1 An overview of freely accessible retinal databases with a semantic segmentation ground truth

Database	Year	Image resolution	Total images	Classification of images	Fundus camera	Format
STARE [26]	2000	605 × 700	20	10 normal 10 pathological	TopCon TRV-50 camera at 35° FOV	PPM
DRIVE [185]	2004	768 × 584	40	20 test set images 20 training set images Out of 40 images, 7 are pathological and 33 normal	Canon CR5 non-mydriatric 3-CCD camera with a 45° FOV	JPEG
MESSIDOR [186]	2004	1440 × 960, 2240 × 1488, 2304 × 1536	1200	800 images with pupil dilation, 400 without dilation	Non-mydriatric 3CCD camera (TopCon TRC NW6) at 45° FOV	TIFF
ARIA [187]	2006	768 × 576	212	92 photographs with AMD, 59 photographs with diabetes, 61 control group photographs	Zeiss FF450+camera at a 50° FOV	TIFF
ImageRet [188, 189]	2008	1500 × 1152	219	DIARETDB0: Out of 130 images, 20 are normal and 110 are abnormal images DIARETDB1: 89 images 5 normal, 84 abnormal.	50° FOV fundus camera, with anonymous settings	PNG
REVIEW [190]	2008	3584 × 2438, 1360 × 1024, 2160 × 1440	16	8 high-resolution image set, 4 vascular disease image set, 2 central light reflex image set, 2 kickpoint image set.	Canon EOS D30 at a 50° FOV	BMP and JPEG
DRIONS-DB [191, 192]	2008	600 × 400	110	Not available (N/A)	Color analogical fundus camera, digitized with HP-PhotoSmart-S20 high-resolution scanner	JPEG
ROC Microaneurysms [193]	2010	768 × 576, 1058 × 1061, 1389 × 1383	100	50 test set images, 50 training set images	TopCon NW100 or a Canon CR5-45NM camera at 45° FOV	JPEG
HRF [194]	2009	3504 × 2336	45	15 normal images, 15 DR patients and 15 glaucomatous patients images	CANON CF-60UVi at a 45° FOV	JPEG
VICAVR [195]	2010	768 × 584	58	N/A	TopCon non-mydriatric camera NW-100 model	JPEG
HEI-MED [196]	2012	Not available	169	N/A	Not available	JPEG
DRiDB [197]	2013	720 × 576	N/A	N/A	Zeiss VISUCAM 200 camera at a 45° FOV	BMP
RIM-ONE [184]	2011	Not available	169	118 healthy images divided into: 12 early glaucoma, 14 moderate glaucoma, 14 deep glaucoma and 11 Ocular hypertension (OHT) images	Nidek AFC-210 with a body of a Canon EOS 5D Mark II, 21.1 megapixels	N/A

stream to capture retina and surrounding tissue blood vessel network for the analysis of various eye diseases. It is helpful for screening abnormal vessels and hyperpermeable vessels leading to ocular tumors and central serous

chorioretinopathy, respectively [6]. Figure 1 represents the anatomical structure of the retina, an image taken from the HRF dataset.

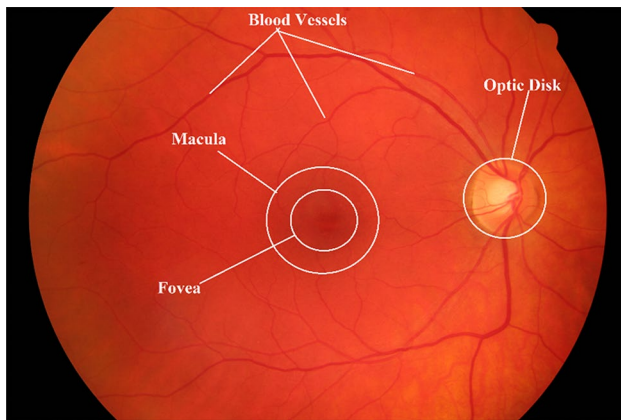


Fig. 1 Anatomical structure of the retina

2.2 Retinal image abnormalities

Various crucial diseases that disturb the retinal vascular network appear in the eye, the cerebrum, or the cardiovascular structure. The following is the outline of the most dominating sicknesses, which can be inspected through retina photograph.

2.2.1 Diabetic retinopathy

Diabetes is a severe, fatal disorder that arises either when the pancreas does not generate sufficient insulin (a hormone that controls glucose), or when the body cannot appropriately handle the insulin it generates [15]. Excess of glucose in blood, a common effect of uncontrolled diabetes, may after sometime lead to severe harm to the heart, eyes, kidneys, blood vessels, and nerves and outcomes in a retinal complication of diabetes called DR [16]. Type 1 and type 2 diabetes are two types of diabetes categorized by the lack of insulin and ineffective use of insulin in the body, respectively. Type 1 diabetes is currently inevitable, and its cause is unknown. Indications of type 1 and type 2 diabetes include constant hunger, vision impairments, excessive urination, weight reduction, tiredness, and thirst [17].

DR is a common complication of diabetes and dominant reason for visual impairments in the people of working age of western nations [18]. Analyzing retinal photographs for the existence of DR to a great extent is a pattern recognition task. The common attributes of DR are MAs, exudates and cotton wool spots, etc. The hyperglycemia in the eye harms the retinal vessel walls. Consequently, new tiny vessels are formed which eventually bleed and damage the retina, a condition called proliferative DR. The damage to the retinal vessel barrier causes fluid leakage, diabetic macular edema (DME) and harm to photoreceptors [13].

2.2.2 Glaucoma

Glaucoma arises when the fluid called aqueous humor inside eye does not drain normally. This fluid piles up and increases pressure inside the eye, which harms the eye's optic nerve that gets worse over time. This can result in visual impairment and blindness [19]. Timely analysis and medication seem to reduce the uncertainty of visual impairment due to glaucoma [2]. Secondary glaucoma is a condition that occurs due to tumor, eye injury, retinal blood vessel blockage, or leakage, swelling of the eye and the use of steroids. The major symptoms of glaucoma are blurred vision, sudden vision loss, and nausea along with extreme eye inflammation. In general, there is no treatment for glaucoma, yet it can be restricted. Eye drops, pills, laser techniques, and surgical operations are utilized to keep or moderate further harm from happening [20].

2.2.3 Cardiovascular disease

Cardiovascular disorder appears in the retina in various ways. Hypertension and atherosclerosis produce variations in the proportion between the width of retinal arteries and veins, famous as the A/V ratio. Narrowing of the arteries and broadening of the veins can decrease A/V ratio and result in an increase in the risk of stroke and myocardial infarction [21]. Moreover, the systemic vascular disorder can lead to arterial/venous occlusions, known as central/branch arterial occlusions (CRAO, BRAO) and central/branch venous occlusions (CRVA, BRVO) [2].

2.2.4 Age-related macular degeneration

AMD is a syndrome that influences individuals beyond 50 years old and is the major source of inevitable vision loss in elderly individuals on the planet [22]. The systemic risk factors consist of male gender, hypertension, hyperlipidemia, chronic kidney disease (CKD), Hepatitis B surface antigen (HBsAg) positivity, liver cancer, coronary heart disease, and increased serum white blood cell levels, etc. [23]. The two noteworthy modes are dry and wet AMD, of which dry AMD ordinarily prompts slow loss of visual acuity. Wet AMD is the most optically dangerous mode, classified by an increase of a choroidal vascular structure into the macula coupled with expanded vascular permeability. The expansion in vascular permeability prompts to unusual fluid collection inside or beneath the retina that result in visual impairments when it associates the middle of the macula [2].

2.3 Openly accessible retinal image datasets

Image datasets possess significant importance in pattern recognition studies, as the developed techniques need to be

validated on sample images. An overview of all the freely accessible retinal image datasets is presented in Table 1. The majority of retinal vessel extraction techniques are assessed on two openly available standard datasets, namely DRIVE and STARE.

3 Categorization of retinal image vessel extraction algorithms

This survey classifies retinal vessel extraction techniques based on the image processing approaches applied and the systems utilized. The retinal vessel extraction methods are classified into five core classes: (I) pattern recognition (PR) approaches, (II) vessel tracking/tracing-based methodologies, (III) model-based techniques, (IV) hardware implementation-based approaches, and (V) hybrid approaches. Some of these classifications are further isolated into subsections. A graphical representation of the classification of retinal blood vessel extraction techniques is shown in Fig. 2.

This review consists of 149 articles considered from peer-reviewed journals. The articles categorized in each of the aforesaid classifications are outlined in Fig. 2 for reference. The categorization has been performed based on the image processing methodology utilized for retinal vessel

extraction. The structure of retinal vessels provides important information for ophthalmologists. Sections 3.1–3.5 provide a detailed explanation of the techniques given in Fig. 2 alongside their analytical discussion.

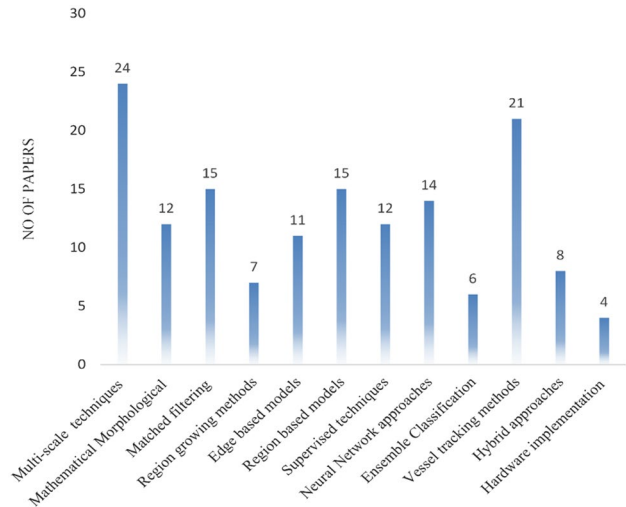


Fig. 3 Classification of papers based on techniques used for retinal vessel extraction

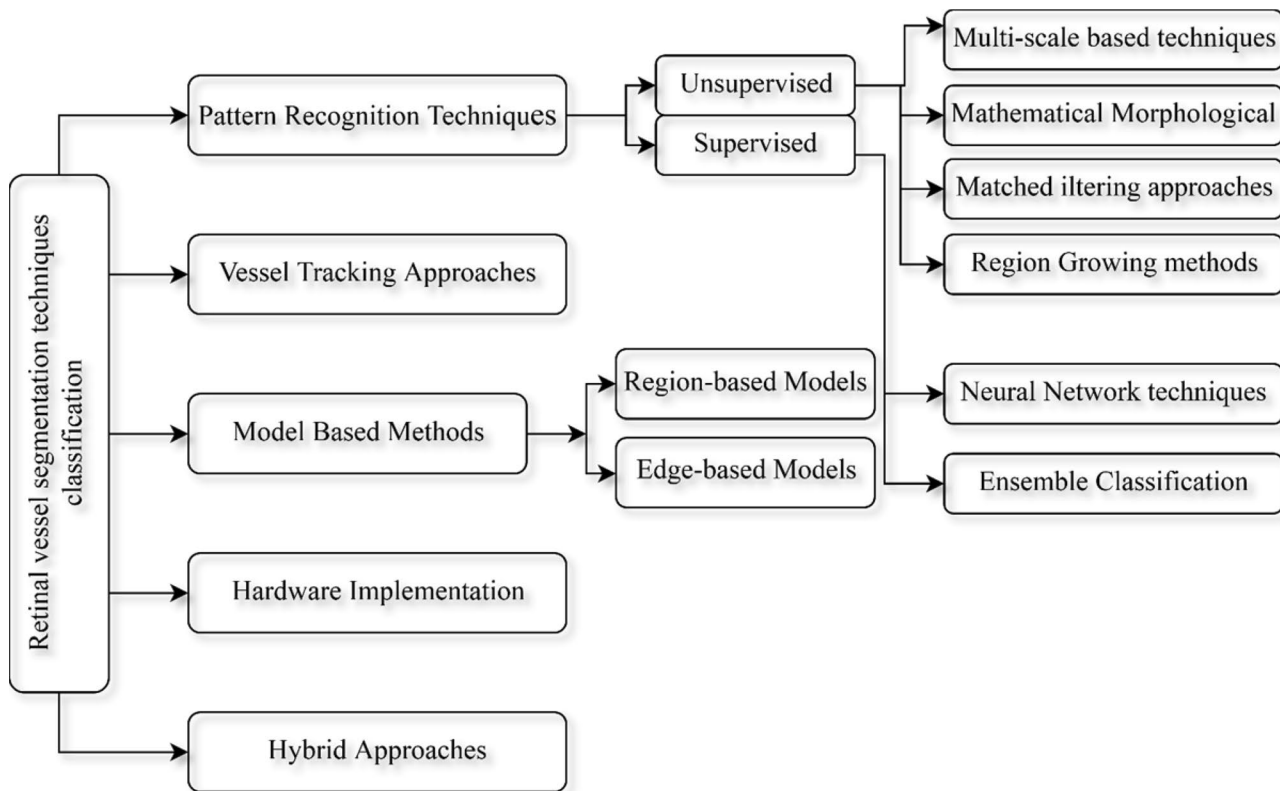


Fig. 2 Classification of retinal vessel segmentation techniques

Figure 3 indicates the number of the papers in each sub-category of retinal vessel extraction techniques. The yearly decomposition of selected papers is shown in Fig. 4.

The performance metrics for retinal vessel detection techniques is summarized in Table 2.

3.1 Pattern recognition approaches

There are PR techniques to handle the identification of patterns and consistency in data. In the vessel segmentation scenario, PR approaches handle the identification of retinal vasculature, vessel attributes, and other background segments. PR algorithms are distributed into two groups: supervised and unsupervised techniques. Supervised approaches exploit some prior marked statistics to isolate vessel and non-vessel pixels, while unsupervised approaches achieve the vessel extraction without any prior marking information. PR unsupervised approaches for retinal vessel extraction are further classified into four groups: (1) multiscale-based techniques, (2) mathematical morphological methods, (3) matched filtering approaches, and (4) region growing methods. Supervised approaches are further categorized into two classes: (1) neural network-based approaches and (2) ensemble classification.

3.1.1 Unsupervised approaches

Multiscale-based techniques Multiscale techniques are based on the variation of image scales to perform vessel extraction. The fundamental point of interest of this procedure is to increase the execution speed. In multiscale approaches, a scale space is generated from the input image for extracting different structures. Major vessel structures are

Table 2 Performance metrics for retinal vessels extraction

Metrics	Explanation
True positive rate (TPR)	TP/Number of vessel pixel
False positive rate (FPR)	FP/Number of background pixel
Sensitivity (Sn)	TPR or TP/(TP + FN)
Specificity (Sp)	1-FPR or TN/(TN + FP)
Accuracy (Acc)	(TP + TN)/(TP + FP + TN + FN)
Area under the ROC Curve (AUC)	$Sn + Sp/2$

segmented from low-contrast photographs, while fine vasculatures are detected from high-contrast ones which increased robustness. Multiscale methods are frequently utilized in vessel extraction in order to address the issue of vessel width variation in fundus images. The articles categorized in the aforesaid classification are outlined in Table 3 for reference.

Frangi et al. [24] proposed vessel enhancement filtering process based on geometrical attributes. The filtering process searches for geometrical attributes with elongated structure. Vessels contrast enhancement is achieved by computing all eigenvalues of the Hessian matrix of the image. A multiscale approach is used due to variation in vessel width. The vesselness measure can be utilized as a preliminary step for vessel extraction of this type of photographs, which is further used for contrast enhancement and detection of tiny vessels [25]. This algorithm introduced a new LRV test in place of Hessian and MF, used in [26]. The LRV is constructed from a 6-D measurement array of MFR and edge responses and their associated confidences. A multiscale MFR are combined to segment vessels with varying size. The edge responses are helpful in differentiating between offset

Fig. 4 The yearly distribution of the selected articles

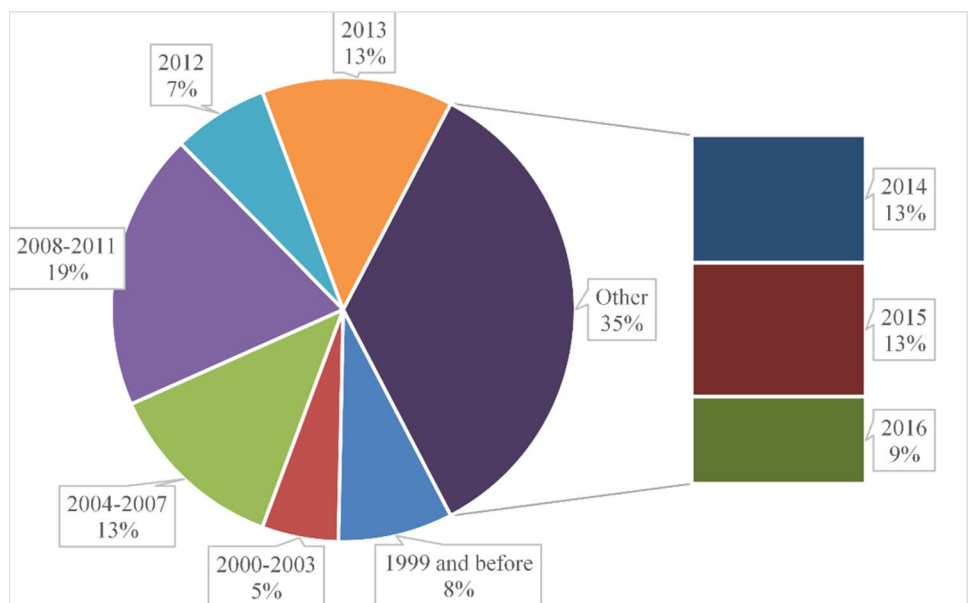


Table 3 Multiscale-based retinal vessel segmentation approaches summarization

References	Year	Techniques	Results for medical examination and applications
Frangi [24]	1998	Eigenvalues evaluation of the Hessian	Vessel width estimation, suitable for noise and background suppression
Martínez-Pérez [27]	1999	Scale-space representation, first and second derivative and region growing (RG) procedure	Adjust contrast variations, applicable to hypertensive patients images
Sofka [25]	2006	Likelihood ratio vesselness (LRV) with matched filter responses (MFR), confidence and edge measures	Detection of narrow and low-contrast vessels, reduction in FPR
Martínez-Pérez [28]	2007	Multiscale feature extraction, RG procedure	Adjust contrast variations, vessel width and branching angle measurement
Farnell [29]	2008	Multiscale line operators (MSLO)	Suitable for diabetic and AMD patients images
Vlachos [30]	2010	Multiscale single channel line tracking algorithm (MSLTA)	Robust to normal and additive Salt and Pepper noise images
Li [31]	2012	Multiscale Production of the Matched Filter (MPMF) responses	Detection of small and weak vessels, vessels width estimation
Moghimirad [32]	2012	Weighted 2-D medialness function, vessel centerline extraction	Vessels radii estimation, robust to noisy and abnormal images
Yu [33]	2012	Second derivatives of Gaussian filtered image at numerous scales, second-order local entropy thresholding	Lesion detection in DR screening, cardiovascular diseases prediction
Nguyen [35]	2013	Multiscale line detection	Vessels widths computation, detect arteriovenous nicking for cardiovascular disease
Fathi [36]	2013	Complex continuous wavelet transform (CCWT), region growing, adaptive histogram-based thresholding	Vessel diameter approximation
Azzopardi [37]	2013	Trainable Combination Of Shifted Filter REsponses (COSFIRE)	Applied to get information about texture, color, contours, and motion
Akram [38]	2013	Multilayered thresholding approach	Identification of diabetic retinopathy
Wang [39]	2013	Matched filtering with multiwavelet kernels (MFMK)	Accurate noise estimation
Ganjee [40]	2014	First-order Derivative of Gaussian (FoDoG) and multi-scale matched filter	Microaneurysms detection in pathological images
Mapayi [42]	2014	Adaptive thresholding method based on local homogeneity information	Additive Gaussian noise removal, applicability to detect blood vessels
Ravichandran [43]	2014	CLAHE, 2-D Gabor filter response, local entropy-based thresholding	Fast contrast enhancement and applicability to detect blood vessels
Annunziata [44]	2015	Multiscale Hessian eigenvalue analysis, percentile-based thresholding	Vessels detection in presence of exudates and other abnormalities
Fraz [46]	2015	QUARTZ (Quantitative Analysis of Retinal Vessel Topology and size)	Glaucoma and proliferative DR detection
Bao [47]	2015	Cake filter	Detect low-contrast and tiny vessels
Kar [48]	2016	Curvelet transform and kernel-based FCM MFR, Laplacian of Gaussian filter (LoG)	Vessels extraction from noisy and pathological retinal images
Emary [49]	2016	Flower pollination search algorithm (FPSA), pattern search (PS) method, possibilistic fuzzy C-means (PFCM)	Robust to healthy and pathological retina images
Al Shehhi [50]	2016	Black top hat (BTH), Graph cut and segmentation, Dijkstra shortest path and segmentation	Tolerant to noisy images, detect small and tinny vessels
Khan [51]	2016	Hessian matrix and eigenvalues approach, Otsu thresholding	Robust to noisy and pathological images, detect tiny vessels

boundaries near abnormalities and genuine vessels. The confidence measures give priority to the contour of the intensity surface rather than the magnitude of the responses, improving the capacity of the LRV to distinguish low-resolution vessels. The six-component dimension arrays are recorded to compute the resultant LRV utilizing pdf's learned from training information. Each component is intended to fix the

issue of identifying tiny and low-resolution vessels, while preventing responses to other retinal photograph segments. Finally, the new LRV is utilized by vessel tracing scheme to extract a complete network of vessel centerline.

Martínez-Pérez et al. [27] coupled processes of the scale-space representation, first and second derivatives of the intensity image and region growing technique. The

scale-space representation provides detail about diameter, elongated structure, and directions of retinal vessels. Two significant statistical attributes of elongated structures depend on the first and second derivative data which provide weights to pixels with a high probability of relating to vessels. The region growing approach permits vessels to grow where the values of the maximum principal curvature lie within a wide interval, and the growth is restricted into segments with low gradients. This permits fast evolution of regions outside the boundaries. Finally, when the margins between clusters are defined, the technique grows vessel and non-vessel clusters at once without the gradient constraint. This technique is further extended using multiscale feature extraction [28]. They investigate the observations that the intensity of the photograph is relational to the volume of blood in the light track corresponding to that pixel.

The MSLO methodology is presented to segment digital fundus images and suppress noise [29]. This was pursued by thresholding to obtain an initial vessel extraction map that was further refined by utilizing a simple RG method. Results with the application of simple median filter are obtained for comparison with MSLO.

Vlachos et al. [30] presented a novel MSLTA and morphological postprocessing steps for extraction of retinal vascular structure. An optimizing process begins with the approximation of a confidence matrix from a cluster of seeds which is obtained from the image's histogram and proceeds to a particular state of the cross-sectional profile gets to be invalid. The multiscale photograph sketch is estimated after coupling the individual photograph sketches along scales, holding the confidence for each pixel to relate to a vessel. The combination of multiscale line tracking results produces a multiscale confidence image map. The preliminary vessel tree is extracted after map quantization of the multiscale confidence map. Map quantization and median filtering procedures remove noisy lines and connection breaches growing the accuracy of the confidence array. Finally, morphological postprocessing eliminates the residual artifacts.

Li et al. [31] proposed multiscale vessel detection approach by convolving the responses of MF at three different scales, which further enhances the vessels while suppressing the noise. MF exhibit strong responses at the vessels on multiple scales, while the background noise does not show higher response and can be easily suppressed. Further, good width estimation can be easily achieved by suitable selection of scale parameters. The method is suitable for small and tiny vessels detection, concurrent extraction of vessels of variant widths, low computational complexity and easier to implement.

A multiscale weighted 2-D medialness function-based technique has been introduced for extraction of retinal vessels in [32]. This approach consists of three noteworthy steps: vessel medialness detection, vessel midline recognition, and vessel reconstruction. The outcomes of the

medialness function are first convolved by the eigenvalues of the Hessian matrix of the photograph. Next, midlines of vessels are detected utilizing noise elimination and reconnection operations [25]. In conclusion, vessel diameter is computed and retinal vessels are extracted.

Yu et al. [33] introduced a multiscale enhancement and second-order local entropy-based technique for the extraction of retinal vessel tree. After preprocessing, vessel network is produced by calculating the eigenvalues of the second derivatives of Gaussian filtered photograph at different scales [24]. The second-order local entropy thresholding is utilized to extract the vessel tree. Finally, a rule-based decision step is used to compute the geometric shape variance between vessels and background to decrease FPR.

An automatic retinal vessel extraction framework based on multiscale line identification [34] was presented by Nguyen et al. [35]. This approach depends on the variation of the length of a basic line detector in order to achieve multiscale line detectors. Line responses at different scales are linearly coupled to eliminate the drawbacks of each individual line detector and to obtain a final binary image.

A novel multiscale vessel enhancement and segmentation technique using a complex continuous wavelet transform (CCWT) is proposed by Fathi et al. [36]. The CCWT differentiates the elongated elements from the boundary structures utilizing real and imaginary parts of the applied wavelet. The resultant binary image is segmented by integrating the modulus values of the wavelet coefficients in the appropriate scales and utilizing an adaptive thresholding technique along with suitable length filtering.

Azzopardi and Petkov presented a trainable COSFIRE filters for detection of vascular junctions in the DRIVE dataset retinal photographs [37]. The setup of a COSFIRE filter relies upon the spatial procedure of contour measures that exists along concentric circles of given radii around a stated ROI. Gabor filters are used for the identification of elongated structures and boundaries. The weighted geometric mean is utilized to combine responses of filters.

Akram and Shoab introduced a novel multilayered thresholding approach for detection of retinal vascular network [38]. The vessels contrast is boosted by utilizing 2-D Gabor filter. The vessel extraction mask is produced utilizing multilayered thresholding approach which traces vessel boundaries and inspect their connectivity by using various thresholds iteratively. Moreover, it removes all false boundaries and vessel segments prior to vessel tracking.

To enhance the vessels, MFMK algorithm is used [39]. A multiscale hierarchical decomposition is utilized on the normalized enhanced photograph to remove the noise and localize vessels. The final binary vessel tree is extracted by using local adaptive thresholding.

Ganjee et al. [40] proposed an enhanced retinal vessel extraction technique depend on high level features

for abnormal photographs. The initial vessel network is detected based on low level features using multiscale MFR [41]. The final binary vessel map is obtained based on high level features.

A new adaptive thresholding method that depends on local homogeneity information for extraction of the retinal vascular network is presented in [42]. Image enhancement and sharpness is performed by using the Unsharp filter, which is pursued by an average filter for smoothening the image. The vessels are localized by utilizing adaptive thresholding depend on local homogeneity information. A combination of morphological postprocessing steps is used on the inverted thresholded photograph to remove the remaining misclassifications.

Ravichandran and Raja [43] proposed a local entropy-based thresholding approach for identification of retinal vessel network. The retinal image is enhanced by applying CLAHE followed by wiener filtering to eliminate background noise. The 2-D Gabor filter is applied for further vessel enhancement. Finally, thresholding is applied to obtain a binary map.

A novel unsupervised retinal vasculature extraction technique that contains inpainting filter, called neighborhood estimator before filling, is exhibited to inpaint exudates in a way that adjacent FPR are considerably decreased during vessel enhancement [44]. The preprocessing steps are adapted from [45]. Multiscale Hessian eigenvalue approach is used for retinal vascular enhancement. Finally, percentile-based thresholding is used to obtain binary image.

Fraz et al. [46] designed a novel QUARTZ approach depending on multiscale line detector for handling and evaluating of retinal photographs. It contains sections for vessel extraction, diameter computation, and angular variation of the individual vessel midline pixel with sub-pixel accuracy, calculating local vessel direction, OD localization, arteriole/venule categorization, tortuosity computation, and exporting the numerical estimations in different output file formats.

A novel approach based on cake filter for extraction of the retinal vascular network is presented in [47]. This technique first joins the real element of orientation score utilizing the cake filter and joins with the adaptive threshold value to get retinal vessel map.

The curvelet transform and kernel-based FCM framework is suggested by Kar et al. [48] for retinal vessel segmentation and optic disk removal. Retinal vasculature enhancement and denoising is performed by applying curvelet transform. The kernel-based FCM approach is used to localize vessel structure. For pathological images, LoG filter along with matched filtering is also applied to differentiate the step and the ramp-like signal from that of vessel structure.

A new framework for multiobjective retinal vessel classification is a combination of FPSA and PFCM [49]. The

FPSA is applied to localize the retinal vessel network utilizing PFCM fitness function. In the second level of optimization, the attained cluster centers are much enhanced utilizing PS as local search, but now the goal is to find the tinny or vessels with small widths.

Al Shehhi et al. [50] suggested a graph-based method for extraction of retinal vasculature. Preprocessing steps are used to enhance contrast and to create essential features to enhance vessel structure due to the sensitivity of vessel patterns to multiscale/multiorientation structure. Graph-based segmentation is used to reduce computational processing required for region of interest into most semantic objects.

Khan et al. [51] introduced morphological Hessian-based approach for retinal vasculature extraction utilizing region-based Otsu thresholding. The preliminary process consists of CLAHE and morphological operations for contrast enrichment and low frequency noise elimination, correspondingly [52]. The Hessian matrix and eigenvalues are utilized in a novel way utilizing multi scales to excerpt wide and thin vessel-enhanced photographs, separately. The modified form of Otsu thresholding is employed to segment vessel and background pixels from both enhanced photographs. In conclusion, length filtering is utilized to remove the undesirable region/segment, background pixels, disease aberrations, and noise, to acquire a final segmented photograph.

Table 4 shows the performance metrics stated by different multiscale techniques of retinal vessel extraction, with a high accuracy stated by Moghimirad [32] both on the DRIVE and STARE datasets.

Mathematical morphological (MM) approaches The basic idea of morphological approaches is to probe a photograph with a small segment or template known as a structuring element (SE). The SE is placed at all probable positions in the photograph, and it is contrasted with the respective local pixels. A morphological filter will store shapes like its SE shape while modifying different shapes. A morphological filter will store shapes similar to its SE shape while modifying dissimilar shapes. Most morphological filters are successful at eliminating both linear and nonlinear noise forms. The MM-based techniques are summarized in Table 5.

Zana and Klein [53] proposed MM- and curvature evaluation-based scheme for extraction of vessel-like structure. Morphological operations are used to prominent vessels with respect to their morphological attributes, and then, cross-curvature evaluation is utilized to distinguish vessel and background pixels. Ayala et al. [54] presented an average of fuzzy sets by utilizing the average distance of Baddeley–Molchanov and the mean of Vorob'ev. The coupling of Zana's method and Baddeley–Molchanov average produced good results. The vessel extraction operations suggested by Zana and Klien have been reconsidered and revised

Table 4 Performance analysis of multiscale techniques

Method	Dataset	Accuracy	Sensitivity	Specificity	AUC
Martinez-Perez [28]	DRIVE	0.9344	0.7246	0.9655	–
	STARE	0.9410	0.7506	0.9569	–
Farnell [29]	ARIA	–	–	–	0.895
	STARE	–	–	–	0.940
Anzalone [87]	DRIVE	0.9419	0.7286	0.981	–
Vlachos [30]	DRIVE	0.929	0.747	0.955	–
Li [31]	DRIVE	0.9496	–	–	–
	STARE	0.9461	–	–	–
Moghimirad [32]	DRIVE	0.9659	–	–	0.9580
	STARE	0.9756	–	–	0.9678
Yu [33]	DRIVE	0.9426	0.7233	–	–
	STARE	0.9463	0.7112	–	–
	HRF	0.9566	0.7938	–	–
Nguyen [35]	DRIVE	0.9407	–	–	–
	STARE	0.9324	–	–	–
	REVIEW	–	–	–	–
Fathi [36]	DRIVE	0.9581	0.7768	0.9759	0.9516
	STARE	0.9591	0.8061	0.9717	0.9680
Akram [38]	DRIVE	0.9469	–	–	0.9632
	STARE	0.9502	–	–	0.9706
Wang [39]	DRIVE	0.9461	–	–	0.9543
	STARE	0.9521	–	–	0.9682
Ganjee [40]	STARE	0.9536	–	–	–
Mapayi [42]	DRIVE	0.9469	0.7477	0.9679	–
Ravichandran [43]	DRIVE	0.9574	0.7259	0.9799	–
	STARE	0.9550	0.7693	0.9672	–
Annunziata [44]	HRF	0.9581	0.7128	0.9836	–0.9655
	STARE	0.9562	0.7128	0.9836	–
Bao [47]	STARE	0.9624	0.7812	–	–
Kar [48]	DRIVE	0.9616	0.7548	0.9792	–
	STARE	0.9730	0.7577	0.9788	–
Emary [49]	DRIVE	0.9368	0.9378	0.8994	–
Al Shehhi [50]	DRIVE	0.934	0.850	0.944	0.893
	STARE	0.924	0.633	0.950	0.800
	ARIA	0.920	0.746	0.947	0.841
Khan [51]	DRIVE	0.961	0.746	0.980	0.863
	STARE	0.946	0.758	0.963	0.861

employing these new averages. All these operations generate grayscale photographs with improved vessels contrast after low level processing. A binary image is obtained by applying a threshold to this enhanced image. The authors preserve the image acquired before utilizing the final threshold which is assumed as a fuzzy set demonstrating the vessels.

Pixel processing-based technique is presented for retinal vessel segmentation in [52]. This approach consists of three stages: preprocessing stage, vessel midline identification, and vessel extraction. In preprocessing stage, background is normalized and thin vessels are enhanced by utilizing a bank of line detection filters at different

orientations. In second stage, a bank of DoOG filters is used for extraction of vessel centerline followed by an RG process for reconnection of vessel centerline. In the last stage, a modified top hat transform with different SEs is utilized to enhance vessels of variable widths, followed by morphological reconstruction to extract binary vessel map. A final binary photograph is acquired by an iterative seeded RG operation of the centerline photographs with the arrangement of four binary networks.

Yang et al. [55] presented a hybrid technique that consists of combination of MM and a fuzzy clustering technique pursued by a purification process. Morphological top hat

Table 5 Summarization of Mathematical Morphological (MM) based retinal vessel segmentation methods

References	Year	Techniques	Results for medical examination and applications
Ayala [54]	2005	Fuzzy MM	Blood vessels detection
Mendonca [52]	2006	Difference of Offset Gaussian(DoOG) filter, multiscale MM	Tolerant to noisy images, detection of tiny and wide vessels
Yang [55]	2008	MM and fuzzy clustering	Robust to normal and abnormal images
Fraz [56]	2011	Differential filtering and morphological processing	Retinal vasculature extraction
Miri [57]	2011	Fast discrete curvelet transform (FDCT) and multistructure elements morphology by reconstruction	Detection of small and tiny vessels, robust to normal and noisy images
Rossant [58]	2011	Morphological approach, Image fusion	Detection of branch retinal vein occlusions, robust to noisy images
Fraz [59]	2012	Vessel midline identification and morphological bit plane slicing	Tolerant to normal, pathological and central reflex images
Fraz [60]	2013	Morphological Bit Planes slicing and DoOG filter	Retinal vascular map extraction
Xu [61]	2013	Shape-based morphology	Elongation-based shape detection
Sigurðsson [62]	2014	Directional mathematical morphology and fuzzy classification	Isolation of major and minor vessels, robust to noisy images
Imani [63]	2015	Morphological component analysis (MCA) and Morlet wavelet transform (MWT)	Separation of lesions from vessels and handle noise

operation is used for vessels enhancement and noise suppression. The binary vessel map is extracted by fuzzy clustering.

Fraz et al. [56] introduced a differential filtering and morphological processing approach for detection of retinal vessel. The FoDoG is used for detection of midlines. A multidirectional morphological top hat operation is performed to acquire the structure and direction map of the vessel along with bit plane slicing of a vessel-enhanced grayscale photograph. The final binary photograph is obtained by combination of midlines with these maps.

The FDCT and multistructure MM is applied for vessel extraction [57]. The vessel contrast is enhanced by using FDCT, and the boundaries of vessels are identified by utilizing a multistructure morphological operation. The wrongly detected boundaries are eliminated by morphological procedure. Connected components analysis (CCA) is coupled with simple thresholding to obtain a final binary image.

Rossant et al. [58] proposed a morphological approach for quantitative analysis and extraction of retinal images. A morphological filter is used for vessel enhancement, and top hat transformation is utilized to extract two attribute images with prominent vessel contrast. Path opening is used for each attribute image so that the main elongated attributes are preserved, whereas the other ones are suppressed. The final segmentation photograph is achieved by thresholding and fusing the two resultant photographs.

The process of vessel midlines identification and morphological bit plane slicing are coupled by Fraz et al. [59] to segment retinal vessels. The FoDoG filter is utilized for extraction of centerlines in four directions, and then, analysis of derivative signs and derivative values are averaged out. The structure and direction map of vessels is acquired

by using a multidirectional morphological top hat process pursued by bit plane slicing of the vessel-enhanced grayscale photograph. The midlines are coupled with these maps to attain the final binary image.

The modified form of [59] is presented for detection of retinal vessels in [60]. The DoOG filter is employed for vessel centerlines identification, and top hat transformation is used for vessel enhancement. A retinal vessel binary image is produced by a bit plane slicing. An iterative RG algorithm fuses the main skeleton and the photographs acquired from bit plane slicing of vessel direction-dependent morphological filters.

Xu et al. [61] designed a system for detection of retinal vessels that consists of two stages: shape-based morphology and a simplification of current tree-based connected processes. The first stage is used to extract retinal vessels. The second stage is an extension of the constrained connectivity framework to non-increasing constraints.

Automatic retinal vascular segmentation method based on directional morphological operations and fuzzy categorization is presented by Sigurðsson et al. [62]. The extraction of vessel attributes is achieved by applying path openings filter. The resulting attributes are utilized to perform a data fusion task depending on fuzzy set theory. Therefore, pixel categorization can be simply achieved to make a vessel tree.

Imani et al. [63] introduced a combination of MCA and MWT for extraction of retinal vascular network. This framework supposes that individual signal is a linear mixture of many morphological significant elements. The MCA technique with suitable transforms is used to isolate vessel and non-vessel pixels. The MWT is utilized for retinal vessel

enhancement. The final binary image is extracted by adaptive thresholding.

The performance evaluation of the methods based on the MF is shown in Table 6, where the maximum accuracy is shown by Imani et al. [63] for both the DRIVE and STARE databases utilizing MCA technique.

Table 6 Performance metrics for Mathematical Morphology based methodologies

Method	Dataset	Accuracy	Sensitivity	Specificity	AUC
Zana [53]	DRIVE	0.9377	0.6971	–	0.8984
Mendonca [52]	DRIVE	0.9452	0.7344	0.9764	–
	STARE	0.9440	0.6996	0.9730	–
Fraz [56]	DRIVE	0.9430	0.7152	0.9768	–
	STARE	0.9442	0.7311	0.9680	–
Miri [57]	DRIVE	0.9458	0.7352	0.9795	–
Rossant [58]	DRIVE	0.9433	–	0.9788	–
Fraz [59]	DRIVE	0.9430	0.7152	0.9769	–
	STARE	0.9442	0.7311	0.9680	–
Fraz [60]	DRIVE	0.9422	0.7302	0.9742	–
	STARE	0.9423	0.7318	0.9660	–
Xu [61]	DRIVE	0.9413	0.6924	0.9779	–
	STARE	0.9471	0.7149	0.9749	–
Sigurðsson [62]	DRIVE	0.9455	–	–	0.9373
Imani [63]	DRIVE	0.9523	0.7524	0.9753	–
	STARE	0.9590	0.7502	0.9745	–

Matched filtering approaches MF convolves a 2-D template with the retinal photograph for extraction of the vascular network. The template is created to demonstrate an element in the photograph at some anonymous location and direction, and the MFR demonstrates the existence of the element. In order to create the template, the following vessel attributes are considered: vessel elongated structure, bifurcation and branching, crossover points and the vessel width variation. The large size and the utilization of the convolution kernel at various rotations cause a computational complexity. Moreover, the kernel reacts ideally to vessels when the vessel profile matches to the kernel. The retinal background disparity and existence of abnormality in the retinal photograph also upturn the FPR because the abnormality can display the same neighborhood elements as the vessels. A MFR methodology is discovered successful when utilized as a part of any other processing methods. The matched filtering-based algorithms are encapsulated in Table 7.

Chaudhuri et al. [64] extracted retinal vessel tree using a feature identification operator depending on the optical and spatial attributes of vessels. A Gaussian profile is utilized to estimate the shape of the cross section of a vein. The MF is applied to extract piecewise linear regions of retinal vessels. Twelve diverse kernels in all possible orientations are employed to explore the vessel segments. The template is rotated in 15 degree additions to fit into vessels of various directions. The highest MFR is chosen for individual pixel and is thresholded to obtain a resultant vessel map. Finally, postprocessing steps are used to trim and classify the vessel regions.

Table 7 Summarization of vessel tracking methodologies

References	Year	Techniques	Results for medical examination and applications
Chaudhuri [64]	1989	2-D Gaussian matched filter (GMF)	Detection of blood vessels
Zhou [65]	1994	MF technique	Vessels width estimation and tracking
Hoover [26]	2000	MF and threshold probing	Classifications of retinal blood vessels
Gang [68]	2002	Amplitude-modified second-order Gaussian filter	Vessel detection and its width estimation
Jiang [69]	2003	Verification-based multi threshold probing	Robust to normal and abnormal images
Al-Rawi [66]	2007	Improved GMF	Sorting of vessel and non-vessel pixels
Sukkaew [70]	2007	Statistically optimized LoG, skeletonization	Detection of the skeletonized structure
Zhang [67]	2009	Modified MF with double-sided thresholding	Screening of proliferative DR
Cinsdikici [71]	2009	MF and ANT colony method	Extraction of retinal vessels & capillaries
Zhang [67]	2010	MF-first-order derivative of Gaussian (FDOG)	Localization of thick and thin vessels
Amin [72]	2011	Phase concurrency and log-Gabor filter	Real-time blood vessel identification
Kaba [73]	2013	MF and expectation maximisation (EM) scheme	Segmentation of vessels in normal and pathological images
Chakraborti [74]	2015	Self-adaptive MF	Extraction of retinal vessels network
Zhang [75]	2015	Modified MF based on second-order gaussian derivatives (SoGD)	Well-kept crossings and tiny vessels network
Singh [76]	2016	Modified MF using Gumbel probability distribution function (PDF) as its kernel	Tolerant to normal and pathological retinal images

The approach depends on a MF technique combined with a preliminary information regarding retinal vessel attributes to extract the vessel edges, trace the centerline of the vessel, and detect suitable characteristics of medical concern [65]. The computational efficiency in straight vessel clusters is achieved by an adaptive densitometric tracing approach depending on local neighborhood information.

Al-Rawi et al. [66] modified Chaudhuri et al. [64] approach by utilizing a comprehensive search optimization process on the DRIVE dataset to search an optimal parameters for MF size, the standard deviation and threshold limit. This system beats the Chaudhuri et al. framework. Zhang et al. [67] also improved the Chaudhuri et al. [64] MF for retinal vessel segmentation that uses a local vessel cross section evaluation utilizing double-sided thresholding to decrease FPR to nonlinear boundaries.

Hoover et al. [26] designed a technique for the identification of retinal vessels based on local and region-based attributes of vessels utilizing a threshold probing method on an MFR photograph. The approach investigates the MFR photograph and uses thresholding with iterative probing for individual pixel as vessel or background [64]. Pixels that are not categorized as vessels from probes are reprocessed for further probing. The technique is validated utilizing ground truth photographs and evaluated against simple thresholding of the MFR. This approach achieved 15 times decrement of FPR over the simple MFR and up to 75% increment of TPR has been noticed.

The amplitude-modified second-order Gaussian filter is introduced by Gang et al. [68] for retinal vessel extraction. It evidences that the vessel diameter can be approximated in a linear connection with the spreading factor of the matched Gaussian filter when the magnitude coefficient of the Gaussian filter is appropriately allocated. Not only the vessel diameter computation gives the width of retinal vessel, but it is also beneficial for enhancing the MF to increase the TPR. An adaptive local thresholding technique based on a verification-based multi threshold probing approach is designed for vessel extraction [69].

Sukkaew et al. [70] described an automatic process for retinal vessel detection in low-contrast and noisy retinal photographs of premature infants that uses a statistically optimized LoG edge detection filter, Otsu thresholding, medial axis transform skeletonization followed by pruning, and edge thinning for vessel extraction.

Cinsdikici and Aydin [71] proposed a combination of MF and ANT colony technique for retinal vessel extraction. The MF and ANT algorithms are applied in parallel on the preprocessed photograph. The length filtering is used on the combined results to extract the complete vessel map. This approach did not produce fruitful results on the pathological images. The methodology is evaluated on the DRIVE dataset.

The MF reacts not only to vessels but also to background boundaries which will result in an increase of FPR. A novel MF with FDOG is presented by Zhang et al. [41] to address this issue. The combination of the zero-mean Gaussian MF and the FDOG is applied to extract the vessels. The application of different scales make it possible to segment both wide and small vessels, followed by a logical OR operation to fuse the outcomes in an effective manner. The MF-FDOG considerably decreases the FPR created by the MF and identifies many fine vessels overlooked by MF. The MF-FDOG has also the advantage of extraction the vessels in abnormal photographs.

Amin and Yan [72] presented a high-speed retinal vessel extraction technique based on phase congruency which is a soft categorization of vessels and constant to contrast variations. The phase congruency of a photograph is computed by utilizing a set of log-Gabor wavelets, and a final image is acquired by thresholding.

Kaba et al. [73] presented a combination of bias correction, MF and the EM retinal vessel extraction technique. The STARE dataset is utilized for evaluation of normal and abnormal retinal images. A new self-adaptive MF utilizing a nonlinear synergistic arrangement of the vesselness filter and the MF for the extraction of retinal vessel network are proposed in [74].

Zhang et al. [75] described an automatic retinal vessel extraction technique based on new MF using SoGD in so-called orientation scores. By locally matching the multiscale SOGD filters with data in orientation scores, they are able to improve elongated structures positioned in various direction planes accordingly. Both junctions and thin vessels are well-maintained because of the suggested multiscale and multiorientation filtering technique.

A novel MF using Gumbel PDF as its kernel is designed by Singh and Srivastava [76]. The image contrast enhancement is performed by using CLAHE. The MFR image is used as an input to entropy-based optimal thresholding. Length filtering is further used for removing artifacts to generate a final binary image.

Table 8 encapsulates the consequences of different morphological-based retinal vessel extraction methods. A highest accuracy is stated by Al-Rawi et al. [66] and Zhang et al. [75], when tested on the DRIVE and STARE datasets, respectively.

Region growing methods The basic theory of the conventional growth region is to collect pixels that have similar characteristics together to form a region. Its efficiency is based on the location of seed points and growth conditions. On the other hand, the traditional technique requires to select seed points manually in order to guarantee the stability. Because the blood vessels have a very wide gray-level distribution, making the traditional region growing method

Table 8 Performance metrics evaluation of techniques based on matched filtering

Method	Dataset	Accuracy	Sensitivity	Specificity	AUC
Chaudhuri [64]	DRIVE	0.8773	–	–	0.7878
Hoover [26]	STARE	0.9267	0.6751	0.9567	–
Jiang [69]	DRIVE	0.9212	–	–	0.9114
	STARE	0.9337	–	–	0.8906
Al-Rawi [66]	DRIVE	0.9535	–	–	0.9435
Zhang [67]	STARE	0.9497	0.6611	–	–
Cinsdikici [71]	DRIVE	0.9293	–	–	0.9407
Zhang [41]	DRIVE	0.9382	0.7120	0.9724	–
	STARE	0.9484	0.7177	0.9753	–
Amin [72]	DRIVE	0.9191	–	–	0.9360
	STARE	0.9081	–	–	0.9199
Kaba [73]	STARE	0.9450	0.6645	–	–
Chakraborti [74]	DRIVE	0.9370	0.7205	0.9579	0.9419
	STARE	0.9379	0.6786	0.9586	–
	CHASE	0.9304	0.5372	0.9583	–
Zhang [75]	DRIVE	0.9446	0.7744	0.9708	–
	STARE	0.9511	0.7940	0.9707	–
Singh [76]	DRIVE	0.9522	0.7594	–	0.9287
	STARE	0.9270	0.7939	–	0.9140

and binary extraction technique hard to precisely segment the vascular map, for the region growing conditions also, depends on range of the image gray level. If each seed point uses the same threshold value, the growth is easy to stop when the blood vessels become more slender. These category methods are summarized in Table 9.

Ahmad Fadzil et al. [77] proposed a region growing approach using FoDoG to extract retinal blood vessel network. The retinal vascular structure is extracted by using a number of processes containing mean filter, CLAHE, bottom-hat morphological operation, contrast stretching. A seed-based region growing (SRG) and gradient-based

region growing (GRG) are applied for vessel reconstruction. The DRIVE dataset is used for the evaluation of this methodology.

A parallel application for the vasculature extraction of high-resolution retinal photographs is introduced by Palomera-Pérez et al. [78]. This approach depends on a data splitting, which permitted a faster handling of those photographs. Two approaches for data partitioning are presented and evaluated: a horizontal partitioning for attribute extraction, and a mixed (horizontal and vertical) partitioning for region growing. ITK serial version is used for extraction high-resolution retinal images.

Jiang et al. [79] suggested a region growing vessel extraction approach depends on spectrum information. This scheme used Fourier transform on the ROI consisting pf vessel information to acquire its spectrum knowledge, according to which its initial feature direction will be detected. Then, coupled boundary knowledge with initial feature direction records the vessel network middle points as the seed points of RG extraction. Finally, the advanced RG approach with branch-based growth scheme is utilized to extract the vessels. The framework is evaluated on different medical images along with standard retinal datasets the DRIVE and the STARE.

Zhao et al. [80] introduced retinal vasculature extraction depending on level set and RG process. The CLAHE and 2-D Gabor filters are used to improve the blood vessels contrast, and an anisotropic diffusion filter is utilized to eradicate the uneven illumination in the photograph and maintain vessel edges. At the end, the RG approach and a region-based ACM with a level set operation are utilized to identify retinal vessels, and their outcomes are superimposed to obtain the resultant binary image.

A structure-based level set technique with an automatic seed point nomination for detection of retinal vascular map is presented in [81]. Additionally, this approach presents an improved zero-level contour regularization term which is more suitable than the ones presented by other approaches for retinal vessel extraction. The model is

Table 9 Region growing-based retinal vessel segmentation techniques summarization

References	Year	Techniques	Results for medical examination and applications
Fadzil [77]	2007	RG technique based on FoDoG	Detection and restoration of retinal vascular network
Palomera-Pérez [78]	2010	ITK serial implementation, RG technique	Segmentation of high-resolution images
Jiang [79]	2013	RG approach based on spectrum information	Retinal vascular map extraction
Zhao [80]	2014	RG approach and a region-based ACM with level set	Suitable for thin and wide vessels extraction, robust to noisy images
Dizdaroğlu [81]	2014	Structure-based level set approach	Retinal vasculature segmentation of pathological and non-pathological images
Panda [83]	2015	Binary Hausdorff Symmetry (BHS) and Edge Distance Seeded RG (EDSRG) method	Robust to normal and pathological images
Lázár [84]	2015	RG approach and a hysteresis thresholding technique	Detection of retinal microaneurysms

tested on their own dataset [82], as well as openly accessible the DRIVE and the STARE datasets.

An automatic seed identification based on a novel BHS measure and a new EDSRG technique for extraction of the retinal vascular network are proposed by Panda et al. [83]. The BHS approach directly computes a binary symmetry decision at every pixel without the measurement of continuous symmetry map and image thresholding. This framework contains four distinct steps: preprocessing, selection of seed (midline) pixels utilizing the BHS approach, postprocessing to remove false midline pixels, and vessel extraction utilizing EDSRG algorithm. The disadvantage of this approach is dependency on the edge.

Lázár and Hajdu introduced a unique RG technique which utilizes a hysteresis thresholding approach with the response vector similarity of contiguous pixels [84]. The performance comparison of different RG algorithms is summarized in Table 10. A maximum accuracy is reported on the DRIVE dataset by Panda et al. [83] and on the STARE dataset by Zhao et al. [80].

3.1.2 Supervised classification

Supervised classification needs hand-marked best quality level photographs for training, and each pixel is depicted by a feature classifier based on neighborhood or global data of the photograph. The constraint for this approach is that an arrangement of main distinctive attributes must be identified for training and characterization techniques. This retinal vascular map is accurately marked by an eye care experts. However, as mentioned in [26], there is noteworthy dissimilarity in the extraction of vessels even among professional graders. As supervised techniques are modeled depending on prior information, their efficiency is generally higher than that of

unsupervised ones and can show superior consequences for normal fundus photographs. The supervised classification methods are listed in Table 11.

Niemeijer et al. [10] excerpt a feature array for every pixel that contains of the green channel of the color photograph and the reactions of a Gaussian MF and its first- and second-order derivatives at multiple scales of pixels. Subsequently, the kNN technique is used to compute the probability of the pixel relating to a vessel [85]. The resultant vessel map is acquired by thresholding the probability map.

The 2-D Gabor wavelet technique for extraction of retinal vessel network is suggested by Soares et al. [86]. It utilizes a feature array made of the pixel’s magnitude, and 2-D Gabor wavelet transform responses are captured at various scales. A GMM classifier is utilized to isolate every pixel as either a foreground or background pixel.

Ricci and Perfetti [34] proposed segmentation of retinal vascular map by utilizing line operators and SVM. A line detector is used on the green plane of a color photograph, and the response is thresholded to acquire unsupervised pixel sorting. Additionally, two orthogonal line detectors are also used along with the gray level of the target pixel to extract a feature array for supervised sorting utilizing an SVM. Comparing with other supervised approaches, the methodology (1) needs less features, (2) feature localization is computationally simpler, and (3) less samples are required for training.

Anzalone et al. [87] designed a modular system for the identification of retinal vessels. The vessel enhancement scheme is adopted from [28]. This method consists of two core blocks: The first block is responsible for contrast enhancement by applying CLAHE, while the second block performs thresholding and some cleaning steps to extract the binary image.

Table 10 Performance metrics for comparison of region growing algorithms

Method	Dataset	Accuracy	Sensitivity	Specificity	AUC
Ahmad Fadzil et al. [77]	DRIVE	0.91–0.95	0.91–0.95	0.88–0.94	–
Palomera-Pérez et al. [78]	DRIVE	0.924	0.779	–	–
	STARE	0.922	0.660	–	–
Jiang et al. [79]	DRIVE	0.9214	–	–	–
Zhao et al. [80]	DRIVE	0.9477	0.7354	0.9789	–
	STARE	0.9509	0.7187	0.9767	–
Dizdaroğlu et al. [81]	DRIVE	0.9365	0.7704	0.9613	–
	STARE	0.9441	0.6926	0.9726	–
	Local	0.9567	0.5179	0.9810	–
Panda et al. [83]	DRIVE	0.9539	0.7337	0.9752	–
	STARE	0.9424	0.8403	0.9547	–
	HRF	0.9420	0.8159	0.9525	–
Lázár and Hajdu [84]	DRIVE	0.9458	0.7763	–	–
	STARE	0.9492	0.7248	–	–
	HRF	0.9572	0.7736	–	–

Table 11 Encapsulation of supervised retinal vessel segmentation techniques

References	Year	Techniques	Results for medical examination and applications
Niemeijer [10]	2004	Gaussian derivative and k-nearest neighbor (kNN) classifier	Localization of blood vessels for retinal disease screening system
Staal [85]	2004	Image ridges and kNN classifier	Automated screening for DR
Soares [86]	2006	Gabor filter and Gaussian mixture model (GMM) classifier	Detection of neovascularization
Ricci [34]	2007	Line operator and support vector machine (SVM)	Robust to normal, noisy and central reflex images
Anzalone [87]	2008	Scale-space analysis and parameter search	Detect vessels from normal and pathological images
Osareh [88]	2009	Multiscale Gabor filter and GMM classifier	Consistent performance for healthy and unhealthy images, Screening of DR
Xu [89]	2010	Wavelets, Hessian matrix and SVM	Detection of major and minor vessels
Lupaşcu [90]	2010	Feature-based AdaBoost Classifier (FABC)	Vasculature structure suitable for clinical applications, robust to noisy images
You [91]	2011	Radial projection and semi-supervised scheme utilizing SVM	Detection of low-contrast and narrow vessels, false detection and overestimate
Varnousfaderani [92]	2015	Multiscale, multiorientation Leung–Malik filter bank	Detection of retinal pathologies such as lesions and anatomical structures
Roychowdhury [93]	2015	Preprocessing, GMM classifier with 2-Gaussians	Detection of intra-retinal micro-vascular abnormalities (IRMA) or vessel beading, neovascularization, and red lesions
Orlando [94]	2016	Discriminatively trained fully connected conditional random field (FC-CRF) model	Detection of DR, vessels width and caliber estimation

Osareh and Shadgar [88] utilized Gabor filters at different scales for vessel extraction, and the attributes are detected utilizing PCA. The elements for Gabor filters are excellently adjusted by conducting tests. The image components are categorized as vessels and background utilizing the corresponding feature arrays by the GMM and SVM classifiers.

For vessels detection, an arrangement of different image processing methods with SVM classifier is presented by Xu and Luo [89]. After preprocessing, the input photograph is further handled by wavelets at different scales for feature abstraction. The line detectors are utilized to detect tiny vessels. A 12-D feature array for individual residual pixel in the binary retinal photograph excluding large vessels is generated. SVM is utilized to differentiate thin vessel regions from the background. A tracing algorithm depends on the coupling of vessel orientation, and the eigenvector of the Hessian matrix is utilized for thin vessel growth to acquire a vessel map.

FABC-based approach is proposed for automatic detection of retinal vascular network [90]. They used a 41-D feature array utilizing statistics of the local intensity arrangement, spatial attributes, and geometry at different measures. Categorization depends on the FABC trained on ground truth patterns of vessel and background pixels. This methodology is validated on the DRIVE dataset.

You et al. [91] introduced an arrangement of the radial projection and the semi-supervised self-training technique utilizing SVM for vessel extraction. The radial projections are used for the localization of vessel midlines, the tiny and

low-contrast vessels. The vessel contrast is enhanced by an improved steerable complex wavelet. The SVM classifier is utilized to detect the main attribute of vessels. The extracted vascular map is acquired by the combination of the two. The methodology is very efficient in extracting tinny and poor resolution vessels but prone to inaccuracies in case of abnormalities.

A new supervised technique to investigate the performance of Leung–Malik filters in classifying retinal vessels is presented by Varnousfaderani et al. [92]. It consists of two-level hierarchical learning framework to extract vessels in abnormal fundus photographs. The retinal disorders, vessels, and non-vessels are demonstrated by expert classifiers in the first level. The results of the expert classifiers are combined to identify vessels in the second level. Roychowdhury et al. [93] suggested a novel three-step retinal vessel extraction algorithm. In the first step, the green channel of a retinal photograph is preprocessed to segment a binary photograph after high-pass filtering, and other binary photograph from the morphologically reconstructed enhanced image for the vessel regions. Subsequently, the mutual segments of both binary photographs are considered as the major vessels. In the second step, all residual pixels in the two binary photographs are categorized by utilizing a GMM classifier. In the third postprocessing step, the major segments of the retinal vessels are coupled with the categorized vessel pixels.

Orlando et al. [94] introduced a discriminatively trained FC-CRF model for extraction of retinal vessels. Attributes of this approach are trained without any human

intervention by utilizing a structured output SVM. This methodology is capable of reconstructing the retinal vessel network very accurately than other conventional CRF by using features detected from the images and fully connected pairwise potentials.

The performance comparison of supervised techniques of retinal vessels is demonstrated in Table 12, where an assessment according to accuracy, the Lupaşcu et al. [90] is exposed to beat the other compared techniques on the DRIVE dataset, while Ricci and Perfetti [34] achieved maximum accuracy on the STARE dataset.

Neural network approaches The benefit of utilizing CNN-based approaches is that it reduces the computational cost due to massively parallel processing. It has also appropriate for hardware application on a chip-set architecture based on the CNN Universal Machine (CNNUM) paradigm. Table 13 shows summary of the neural network-based methods.

ANNs have been widely inspected for extracting fundus images attributes such as the vessel structure and perform categorizations which depend on geometric probabilities rather than objective reasoning [95]. Sinthanayothin et al. [96] proposed MLP-NN for extraction of retinal vessels depends on the inputs from a PCA of the photograph and boundary recognition of the intensity. The results of this approach are compared with the manually labeled retinal components by an expert ophthalmologist.

A back propagation technique for the extraction of vessels in angiography is presented by Nekovei and Ying [97]. This approach uses NN directly to pixels without prior attributes extraction. The pixels of the small sub-window, which slides across the angiogram photograph, are directly fed as input to the network. The gold standard photographs of hand-marked angiograms are utilized as the training set to set the network’s weights. An improved form of the common delta-rule is utilized to acquire these weights.

Yao and Chen [98] introduced a PCNN and fast 2-D Otsu approach for detection of retinal vascular network. The binary vessel map is acquired via evaluating region-based attributes. The STARE dataset is used for performance evaluation of this method.

Lupaşcu and Tegolo [99] proposed an unsupervised neural network self-organizing map (SOM) and K-means clustering approach for retinal vasculature extraction. AdaBoost classifier is used to divide map units into two groups [90]. SOM and K-means clustering produces good results on a small number of classes and is also very fast. This framework is tested on the DRIVE dataset.

A new supervised scheme based on neural network (NN) is proposed by Marin et al. [45] for extraction of retinal vasculature. This technique utilizes a 7-D feature array that depends on gray-level and moment invariant-based attributes. A multilayer feed forward NN is used for training and categorization. The NN is trained on the DRIVE dataset only, but it shows robustness with various image settings and on different image datasets.

Table 12 Performance comparison for supervised approaches

Method	Dataset	Accuracy	Sensitivity	Specificity	AUC
Niemeijer [10]	DRIVE	0.9416	0.7145	–	0.9294
Staal [85]	DRIVE	0.9442	–	–	0.952
	STARE	0.9516	–	–	0.9614
Soares [86]	DRIVE	0.9466	–	–	0.9614
	STARE	0.9480	–	–	0.9671
Ricci [34]	DRIVE	0.9563	–	–	0.9558
	STARE	0.9584	–	–	0.9602
Osareh [88]	DRIVE	–	–	–	0.9650
Xu [89]	DRIVE	0.9328	0.7760	–	–
Lupaşcu [90]	DRIVE	0.9597	–	–	0.9561
You [91]	DRIVE	0.9434	0.7410	0.9751	–
	STARE	0.9497	0.7260	0.9756	–
Varnousfaderani [92]	DRIVE	0.903	–	–	0.955
	STARE	0.927	–	–	0.971
Roychowdhury [93]	DRIVE	0.952	0.725	0.983	0.962
	STARE	0.951	0.772	0.973	0.969
Orlando [94]	DRIVE	–	0.7897	0.9684	–
	STARE	–	0.7680	0.9738	–
	CHASEDB1	–	0.7277	0.9712	–
	HRF	–	0.7874	0.9584	–

Table 13 Summarization of neural network-based retinal vessel segmentation methods

References	Year	Techniques	Results for medical examination and applications
Akita [95]	1982	Artificial neural networks (ANNs)	Highlighted ocular fundus images issues related to hypertension and diabetes
Nekovei [97]	1995	Back propagation NN	Detection of vascular map in angiograms
Sinthanayothin [96]	1999	Multilayer perceptron neural network (MLP-NN)	Localization of the optic disk, blood vessels and the fovea
Yao [98]	2009	Pulse coupled neural network (PCNN) and fast 2-D Otsu	Blood vessel extraction in normal images
Marin [45]	2011	Neural network based on gray level and moment invariant-based features	Tolerant to different datasets, robust to normal and noisy images, detection of DR
Vega [100]	2013	Lattice neural networks with dendritic processing (LNNDP)	Remove noise and false positives
Andersson [103]	2013	Modified gradient decent based on artificial neural network (ANN)	Segmentation of blood vessels, tolerant to noisy images
Anitha [104]	2013	Efficient Kohonen fuzzy neural (EKFN) network	Pathology detection in retinal images
Franklin [105]	2014	ANN approach based on Gabor and moment invariants-based features	Screening of DR, localization of retinal vasculature
Vega [101]	2015	Modified LNNDP	Robust to normal and pathological images
Li [106]	2015	Cross-modality learning algorithm	Consistent to noisy and abnormal images, Analysis of ophthalmologic disorders
Sironi [107]	2015	Learning-based filtering	Extraction of curvilinear structures
Ceylan [108]	2016	Complex ripplelet-I transform and complex valued ANN	Extraction of vascular network
Liskowski [109]	2016	Deep neural network approach	Resistant to the phenomenon of central vessel reflex

A supervised framework based on different settings of NN known as LNNDP is suggested by Vega et al. [100]. Pre-processing, feature extraction, classification, postprocessing are the major steps of this approach. The LNNDP approach is different from the conventional NN approaches in the computation executed by the single neuron. The STARE data are used for validation of this methodology. Vega et al. [101] proposed another adapted version of the hyperboxes partition technique [102] for detection of retinal vasculature. The LNNDP an advance version of [100] is used for extraction of retinal vessels.

Andersson et al. [103] introduced modified gradient descent (MGD) search for level set-based detection of retinal blood vessels. This approach used two MGD approaches: One utilizes a momentum term, and others depends on resilient propagation (Rprop). The MGD approaches are utilized to train the learning systems based on ANNs. The framework is validated on the real and synthetic data. The DRIVE dataset is used for retinal vessel extraction.

Anitha and Hemanth [104] suggested an EKFN-based automatic technique retinal detection of retinal vascular map. This automatic approach also contains hybrid feature detection methods which considerably enhance the competence of the proposed NN. This system is tested on their own collected datasets.

The ANN-based approach is proposed by Franklin and Rajan [105] to detect retinal vasculature. The MLP-NN is used for identification of retinal blood vessels, for which

the inputs are obtained from Gabor and moment invariants-based features. The disadvantage of this approach is missing of tiny blood vessels in some cases. The images from the DRIVE dataset are used for confirmation and evaluation of this methodology.

A novel supervised technique for retinal vasculature extraction is redesigned as a cross-modality data transformation problem [106]. A wide and deep NN with robust training aptitude is presented to model the transformation, and an efficient training tactic is used. The segmentation process does not require artificially designed features, reducing the influence of particular features. This approach is also robust to noisy and pathological images.

Sironi et al. [107] introduced a learning-based filtering system used for detection of curvilinear structures along with two learning-based approaches for acquiring separable filter banks. The first one directly learns separable filters by varying the regular objective function. The second one acquires a basis of separable filters to estimate an existing filter bank, and not only acquires the equivalent performance of the original, but also significantly decreases the quantity of filters, and thus convolutions, needed. The performance is evaluated on the DRIVE dataset. The comparison of different techniques based on neural network is shown in Table 14.

Ceylan and Yaşar [108] proposed a complex ripplelet-I transform and complex valued ANN for detection of retinal vascular map. The ripplelet-I transform estimates the features

Table 14 Performance metrics for neural network-based methodologies

Method	Dataset	Accuracy	Sensitivity	Specificity	AUC
Yao and Chen [98]	STARE	–	0.8035	0.972	–
Lupaşcu and Tegolo [99]	DRIVE	0.9459	0.696	0.9702	–
Marin et al. [45]	DRIVE	0.9452	0.7067	0.9801	0.9588
	STARE	0.9526	0.6944	0.9819	0.9769
Vega et al. [101]	DRIVE	0.9412	0.7444	0.9600	–
	STARE	0.9483	0.7019	0.9671	–
Li et al. [106]	DRIVE	0.9527	0.7569	0.9816	0.9738
	STARE	0.9628	0.7726	0.9844	0.9879
	CHASE_DB1	0.9581	0.7507	0.9793	0.9716
Sironi et al. [107]	DRIVE	–	–	–	0.962
Ceylan and Yaşar [108]	DRIVE	0.9844	0.853	–	–
	STARE	0.9803	0.940	–	–
Liskowski and Krawiec [109]	DRIVE	0.9230	0.9241	0.9160	0.9738
	STARE	0.9309	0.9307	0.9304	0.9820
	CHASE_DB1	0.9577	0.8793	0.9668	0.9845

matrix from the retinal images of standard datasets, which is further used as an input to the complex valued ANN. The inverse transformation is applied to resize the output coefficients of ANN.

A novel supervised DNN-based approach is presented for extraction of retinal vascular map [109]. The DNN is trained on a large (up to 400,000) sample of examples preprocessed with global contrast normalization, zero-phase whitening, and augmented using geometric transformations and gamma corrections.

Table 14 demonstrates the performance evaluation for the methodologies based on neural network. The Ceylan and Yaşar [108] reported the highest accuracy on the both standard datasets: DRIVE and STARE.

Ensemble classification approaches Ensemble classification is the procedure by which various classifiers are strategically created and pooled to address a specific machine learning

task. The ensemble classification approaches are listed in Table 15.

Fraz et al. [110] suggested a supervised classification approach utilizing an ensemble classifier of bagged decision trees for extraction of retinal vessels. They utilized decision trees as the categorization model and the outputs of these frail classifiers are pooled by means of bootstrap aggregation also known as Bagging. They utilized 8-D feature array containing the outputs from a filter set comprising the filter templates of dual-Gaussian and Gabor functions and the line strength computation, which deals the central vessel reflex successfully. This approach is further modified utilizing 9-D feature vector for detection of retinal vascular map [111]. The feature vector contains the vessel tree acquired from the orientation investigation of the gradient vector field (GVF), the morphological procedure, line strength computation and the Gabor filter response which translates data to

Table 15 Summarization of ensemble classification-based retinal vessel segmentation methods

References	Year	Techniques	Results for medical examination and applications
Fraz [110]	2012	An ensemble classification system using 8-D feature vector	Resistant to the phenomenon of central vessel reflex and pathological images
Fraz [111]	2012	An ensemble classification system using 9-D feature vector	Robust to normal and pathological retinas, detect cardiovascular risk factors
Fraz [112]	2014	An ensemble classification system using 13-D feature vector	Vessels extraction of pediatric retinal images from different ethnic origins
Wang [113]	2015	Feature and ensemble learning approach, convolutional neural network (CNN) and RF classifiers	Segmentation of retinal blood vessels
Welikala [114]	2016	SVM classifier and ensemble classifier of bagged decision trees.	Creation of vessel morphometric data suitable for epidemiological studies
Zhu [115]	2016	An ensemble classification approach using 36-D feature vector	Suitable for computer-aided diagnosis and disease screening

deal with the both healthy and unhealthy fundus photographs successfully. This concept is further utilized by applying 13-D feature vector containing of the responses from a filters set comprising the filter templates of dual-Gaussian, second-order derivative of Gaussian and Gabor functions, along with the line strength measures and morphological procedure, which deals with the central vessel reflex successfully [112]. The CHASE_DB1 database is utilized for the performance validation of the proposed framework.

A feature and ensemble learning-based technique utilizing a combination of two classifier CNN and RF is proposed [113]. CNN works as a trainable hierarchical feature extractor, and ensemble RFs work as a trainable classifier.

Two different state-of-the-art classifiers SVM and ensemble are explored by Welikala et al. [114]. Both delivered remarkable consequences; however, the SVM classifier is chosen as it marginally left behind the ensemble classifier of bagged decision trees.

Zhu et al. [115] proposed an ensemble approach utilizing 36-D feature vector, consisting of local attributes, morphological procedure with multiscale and multiorientation and DVFs. Then, weak classifiers are trained by the classification and regression tree (CART) utilizing information of a feature array. Lastly, an FABC is created by iteratively training for the retinal vessel extraction.

The performance metrics used for analysis of the efficiency of ensemble classification-based approaches of retinal vessels segmentation are shown in Table 16, where Wang et al. [113] achieved a highest accuracy on the DRIVE and STARE datasets.

3.2 Vessel tracking techniques

The tracking methodologies track the vessels based on manual/automatic selection of some seed positions and subsequently the vessel midline detection steered by local data. The benefit of tracing-based techniques is its competence since only pixels near to the preliminary points are inspected and analyzed. Additionally, significant statistics (i.e., vessel

width and bifurcations) are usually detected along with the vessel tree. However, a disadvantage of such techniques is that refined approaches have been introduced due to the complex intensity profile at branching or crossover positions. Since vessel bifurcation or boundary locations are not well modeled, this process often tends to end at these positions and this leads to incompleteness in the extraction result. Table 17 shows the summary of all vessel tracking based frameworks.

Recursive tracking-based vasculature extraction in retinal angiograms is presented in [116]. Initially, choosing the starting point and direction, a section within vessel map is identified. After identification of segment, it is discarded in the angiogram photograph. The recognition-elimination plan is utilized to overcome the issue of tracking-path re-entry in those zones where vessels crossover happens. This operation is executed repeatedly to excerpt the retinal vessel network. Human intervention is involved in this approach to identify vessel seed points. An automatic vessel tracking technique is proposed by Liang et al. [65] to detect vessel segment and tortuosity. The method depends on a MF technique along with a preliminary information about retinal vessel attributes to automatically extract the vessel edges, centerline, and other helpful information of clinical interest. However, this approach requires human interference for selection of direction, start and end points.

Chutatape et al. [117] utilizes a combination of Gaussian and Kalman filters for retinal vessel extraction. The second-order Gaussian MF is used to detect the vessel midline center point, and then, the tracing operation is performed, initializing from the boundary of the OD. The Kalman filter is utilized to detect the subsequent vessel segment position utilizing all the former and the current segment attributes.

Tolias and Panas [118] proposed a retinal vessel tracking framework based on the FCM clustering approach. The remarkable characteristics of this approach are that it does not use any boundary data to trace the precise position of the vessels and in result suppressed the noise. Also, the method utilizes only fuzzy image intensity data. Additionally, there

Table 16 Performance comparison of the ensemble classification methods

Method	Dataset	Accuracy	Sensitivity	Specificity	AUC
Fraz et al. [110]	CHASE_DB1	0.9473	0.7106	0.9729	0.9740
Fraz et al. [111]	DRIVE	0.9480	0.7406	0.9807	0.9747
	STARE	0.9534	0.7548	0.9763	0.9768
	CHASE_DB1	0.9469	0.7224	0.9711	0.9712
Fraz et al. [112]	CHASE_DB1	0.9524	0.7259	0.9770	0.9760
Wang et al. [113]	DRIVE	0.9767	0.8173	0.9733	0.9475
	STARE	0.9813	0.8104	0.9791	0.9751
Welikala et al. [114]	UK Biobank	–	0.9533	0.9113	0.9828
Zhu et al. [115]	DRIVE	0.9618	0.7462	0.9838	–
	RIS	0.9535	0.8319	0.9607	–

Table 17 Summarization of matched filtering-based retinal vessel segmentation methods

References	Year	Techniques	Results for medical examination and applications
Liu [116]	1993	Recursive tracking	Vascular map extraction in angiograms
Liang [65]	1994	MF-based iterative tracking with human interference	Stenosis and occlusion detection of a vessel, diameter measurement
Chutatape [117]	1998	Gaussian and Kalman filters	Detection of complete vessels network
Tolias [118]	1998	Fuzzy C-means (FCM) clustering	Handles efficiently junctions and forks
Ali [119]	1999	Recursive tracking with directional templates	Tracking of retinal vascular map and exploration of joints and crossovers
Lalonde [120]	2000	Non-recursive paired tracking	Suitable for handling of bifurcations, broken edges and noise
Quek [121]	2001	Wave propagation and traceback	Detection of vascular network from angiography images
Delibasis [122]	2010	Model-based tracking	Extraction of entire vessel map, estimation of vessel's width
Xu [123]	2011	Graph-based approach	Identification of retinal and cardiovascular diseases
Huang [124]	2012	Modified exploratory algorithm and FCM	Diagnoses of diabetes and hypertension
Yin [125]	2012	Probabilistic tracking approach	Retinal vessels extraction, robust to noise
Nayebifar [126]	2013	Vessel tracking using particle filters	Tracks the thin vessels, tolerant to noise
De [131]	2013	Probabilistic graphical models	Tracking vessels network
Fraz [127]	2013	Model-based technique	Cardiovascular disease detection, estimation of vessel caliber
Yin [128]	2013	Bayesian approach with maximum a posteriori (MAP)	Vessels detection, width computation and vessel structure identification
Bekkers [130]	2014	Vessel Edges Through the Orientation Score (ETOS) and Centerline Tracking through a multiscale set of noninvertible Orientation Scores (CTOS)	Retinal vasculature tracking, approximations of retinal vessel's width
De [132]	2014	Graph-based tracking approach	Handle many crossover scenarios, vessel's tracing
Poletti [133]	2014	Graph search-based vessel tracing	Identification of retinal vascular map, vessel width evaluation
Zhang [134]	2014	MAP criterion and multiscale line tracking	Accurate vessel's tracking
Cheng [135]	2014	Matrix-forest theorem of directed graphs	Tracing vessel's network in retina images
Chen [136]	2015	Anisotropic fast marching-based geodesic technique	Tubular structure extraction

is no setting of parameters and initialization required. The technique tracked the major vessels in the image very well and overlooked only tiny and low-contrast vessels.

Ali et al. [119] presented the recursive tracking depend on recursive tracking of the vessels using directional templates. This approach improves the previous work in different directions: (1) No human intervention is required, only few parametric tuning; (2) it is robust to image contrast variations, major and tiny vessels and artifact elimination, and (3) it does not need the vasculature to be linked. The technique is tested on normal and abnormal dilated retinal images.

Non-recursive paired tracking method is presented to trace the vessels in low-contrast retinal images utilizing their boundary network as calculated by the canny edge detector [120]. Tracing proceeds by subsequent edge line while observing the connectivity of its twin edge. Seed generation permits the approach to handle junctions (a main problem in vessel tracking) and jump over damaged edges. Five typical retinal images are used for the algorithm evaluation.

Quek and Kirbas [121] introduced retinal vascular map detection approach based on a wave propagation and

trace-back scheme. Every vessel pixel is marked on the photograph with the likelihood by applying a dual-sigmoidal filter. The refractive index photograph is created by the complement of this image, and then, a digital wave is circulated through the photograph from the base of the vascular map. The vascular map is acquired by tracking the wave along the neighborhood perpendicular to the waveform. This methodology allows the location of the particular vessels, as well as the vascular connecting morphology also.

A model-based tracking method for vessel extraction and width computation is proposed in [122]. The approach uses a parametric model of a vessel consisted of a 'stripe' which utilizes statistical attributes for parameter descriptions. A measure of match (MoM) computes the resemblance between the model and the input photograph. The starting of seed pixels for vessel tracing is performed utilizing a multiscale filter and distributing the binary output in non-overlapping square chunks and selecting a random nonzero pixel as a seed [24]. This approach does not involve any human interference. The vessel width is additionally recuperated with the characterized model

using the strip width parameter in this way assuming direct reliance between vessel width and model width parameter. The DRIVE dataset as a training set is used for tuning of parameters.

Xu et al. [123] designed graph-based technique for tracking of vessel edges and widths in the retinal photographs. This framework is tested on the REVIEW dataset. This method depends on the initial vessel extraction of the image. FPR or disconnection in the vessels may result in an increase in falsification of edge detection and vessel width computation. This model does not deal with the crossing and branching points separately.

Huang et al. [124] suggested an automatic framework for tracking of retinal vascular network. The approach includes OD position, midline detection of the retinal vascular network, individual network marking, and branch order evaluation. The retinal vessel tree is detected by probing scheme without segmentation. Based on the marked terminal points and OD position, the preliminary position and termination positions for individual retinal vascular network are recognized. In light of the results, morphological properties such as statistical and topological attributes are quantitatively computed, particularly depending on branch order evaluation. The improvement is the identification of the neighborhood statistics of a retinal vessel map. The DRIVE dataset is used for validation of this approach.

A probabilistic tracking framework [125] used Bayesian approach with the MAP criterion for extraction of vessel boundary. Bayesian approach with the MAP criterion is used for extraction of vessel boundary. This approach extracted the vessels efficiently on both synthetic and real retinal photographs and outperforms many conventional vessel extraction techniques. The REVIEW dataset is used for validation of this approach.

The novel technique that depends on particle filtering is presented to track the vessel trajectories in fundus image [126]. The tracking process starts by selecting some preliminary positions within a vessel and remains until the end of the vessel or a branching. In bifurcation, relative to the quantity of branches, the new routes are advised by new preliminary positions. Hence, the methodology contains two stages. In the initial step, the OD position is identified and its nearby impact on biasing gray-level distribution is diminished. At that point, using the distinguished OD, some underlying positions are characterized for the vessel tracing method. In the second step, the tracing is implemented to detect the vessel trajectory utilizing the particle filtering technique.

Fraz et al. [127] designed a model-based approach for computation of vessel caliber from fundus photographs. The initial vascular network is extracted from the vessel probability map photograph. The vessel centerline is detected by using the scale-space skeletonization technique on the binary

extracted image. The 2-D model is used for the measurements of vessel widths. The CHASE DB1 dataset is used for validation of this algorithm.

A probabilistic tracking-based technique for automatic detection of retinal blood vessels is presented in [128]. This is a tracking based-method using a Bayesian technique with MAP as criterion to extract vessel edge points. This method is tested on the STARE and DRIVE datasets. The REVIEW database is utilized for diameter computation of retinal vessels.

A minimal path-based technique is proposed for retinal vessel extraction and A/V classification [129]. It contains two major stages: a local classification of vessel segments utilizing the color data and a tracking process depends on the minimal path technique which links vessel segments in succeeding circumferences. Finally, the classification results of all connected vessels are combined with a voting system. Thus, the local clustering scheme permits to eliminate the influence of the irregular brightness in the clustering, whereas the tracking process gives a way to confirm the growing of a vessel taking into account the color information along the whole vessel. This approach is validated on the REVIEW dataset.

Bekkers et al. [130] introduced a novel framework for extraction of vessel edges through the orientation score (ETOS) of an image. The ETOS approach can generally be utilized with both invertible and noninvertible orientation scores (NIOS), which are constructed with cake wavelets and Gabor wavelets, respectively. The IOS produced good results. Another technique that depends on vessel centerline tracking through a multiscale set of noninvertible orientation scores (CTOS) is also presented. The CTOS method is very fast, and the multiscale technique makes the method less stable at critical vessel points compared to ETOS. The HRF and REVIEW datasets are used for the validation of COTS and ETOS approach, respectively.

De et al. [131] presented probabilistic graphical models for automatic tracking of retinal vasculature. This approach consists of two-phase processes: In first phase, vessel skeleton is extracted through segmentation followed by second stage to track the vessel trajectories and direction through graphical models. This model is tested on the DRIVE dataset. The graph-based method to trace retinal vascular network is extended in [132].

Poletti and Ruggeri [133] suggested a graph search-based retinal vessel extraction. Two different aspects are analyzed in this approach: In the first one, accuracy, sensitivity, and specificity of the retinal vessel extraction are computed on three different datasets: the DRIVE, STARE, and YARD. In the second analysis, diameter is computed using the REVIEW dataset.

Bayesian theory and multiscale line extraction-based approach is presented to track retinal vascular map [134].

There is no human interference in the selection of initial tracking points and direction. The REVIEW dataset is used for validation of this approach. Matrix-forest theorem of directed graphs is presented for detection of retinal vasculature [135].

Chen and Cohen [136] designed anisotropic fast marching-based geodesic approach for detection of midlines of retinal vessel segments and their edges. This approach is associated with geodesic or minimal path algorithm which is specifically capable of detecting an elongated profile, such as a blood vessel. The DRIVE dataset is used for confirmation of this method. The performance results of the vessel tracking methods are shown in Table 18.

3.3 Model-based techniques

Vermeer et al. [137] designed a model-based approach for identification of retinal vessels. The performance of this framework is improved by using Laplace and thresholding segmentation step, pursued by a categorization step. The selection of different datasets affects the accuracy of the technique. The approach is evaluated on GDx generated photographs.

Mahadevan et al. [138] suggested a combination of three systems: Huber’s censored likelihood ratio test, the rank-based algorithms [139] and the robust model selection [140], for vessel extraction in noisy photographs [141]. The approach is flexible to combine a range of vessel profile models containing Gaussian, derivatives of Gaussian and dual-Gaussian and different noise types like Gaussian and Poisson noise. The model is validated on simulated and real data. The outcomes are contrasted with the MF and the direct exploratory vessel tracking approach [132]. An improved version of this vessel extraction model is also presented by the authors with the addition of a generalized dual-Gaussian cross-sectional profile for better-quality extraction of vessels comprising a central vessel reflex [142]. The summarization of model based techniques is shown in Table 19.

The CNN approaches are a fast mechanism for extraction of retinal vasculature due to its massively parallel processing [143]. The major steps consist of CNN-based histogram

equalization and variation, simple adaptive thresholding, and morphological procedure. The MATCNN environment is used for simulation of this methodology. The drawback of this approach is the dependency on different design parameter for opening operator and the varying CNN kernels for the local approximation of the variance. These drawbacks are addressed by a novel CNN-based framework [144] utilizing geometrical information instead of applying generic algorithms [143]. This scheme is validated on the DRIVE dataset.

Extraction of retinal vessels by using multiresolution Hermite model (MHM) is presented by Li et al., which utilizes a 2-D Hermite function intensity model in a quad-tree structure over a range of spatial resolutions [145]. The MHM depends on a Hermite polynomial rather than a combination of Gaussian to integrate the central light reflex [146]. A MHM is coupled with an expectation-maximization (EM) optimization approach and statistical associating technique for the modeling and evaluation of retinal vessel network.

Lam and Yan [147] described a new vessel extraction technique for abnormal fundus photographs that depends on the DVFs. In this approach, the midlines are extracted utilizing the normalized GVF, and then, the elongated vessel-like entities are extracted utilizing the Laplacian operator of a pixel. The false distinguished vessel-like elements are trimmed by separation from extracted midlines.

Alonso-Montes et al. [148] suggested a pixel-parallel methodology for detection of vascular network which is adapted from [149] in terms of neighborhood element convolutions and morphological processes coupled with arithmetic and logical processes to be executed and verified in a fine-grain single instruction multiple data (SIMD) parallel processor array [150]. The outward of vessels is sought by parallel dynamic form, the PLS [151].

Lam et al. [152] presented a regularization-based multiconcavity modeling to deal simultaneously both with the healthy and abnormal retinas with bright and dark abrasions. The differentiable concavity measure is designed to deal with bright lesions. The line-shape concavity measure is presented to take out dim injuries which have a power structure disparate from the lengthened vessels in a retina.

Table 18 Performance metrics analysis for the vessel tracking based approaches

Method	Dataset	Accuracy	Sensitivity	Specificity	AUC
Delibasis et al. [122]	DRIVE	0.9311	0.7288	0.9505	–
Yin et al. [128]	DRIVE	0.9267	0.6522	0.9710	–
	STARE	0.9412	0.7248	0.9666	–
De et al. [131]	DRIVE	0.9429	0.7602	–	–
De et al. [132]	DRIVE	0.9429	0.7602	–	–
Poletti and Ruggeri [133]	DRIVE	0.9356	0.7304	0.9662	–
	STARE	0.9401	0.6923	0.9734	–
	Local	0.9618	0.8258	0.9749	–

Table 19 Summarization of model-based retinal vessel segmentation methods

References	Year	Techniques	Results for medical examination and applications
<i>Edge based models</i>			
Vermeer [137]	2004	Laplacian profile model	Extraction of blood vessels, especially for images with specular reflection
Mahadevan [141]	2004	Robust vessel profile model	Detection of vasculature in noisy retinal video images
Alonso [143]	2005	Cellular neural networks (CNN)	Identification of retinal vascular map
Perfetti [144]	2007	CNN-based technique	Segmentation of retinal blood vessels
Li [145]	2007	Multiresolution Hermite model	Detection of vessel structure, robust to noisy and pathology images
Narasimha-Iyer [146]	2007	Dual-Gaussian profile model	Detection of BRVO disorder, estimate the tortuosity and diameter variations
Lam [147]	2008	Divergence of vector fields (DVF)	Robust to normal, noisy and pathological retina images
Alonso-Montes [148]	2008	Pixel level snakes (PLS), pixel-parallel technique	Localization of retinal vessels network
Lam [152]	2010	Multiconcavity modeling	Remove bright and dark lesions, Robust to normal, noisy and pathological images
Zhu [154]	2010	Log-Gabor filters, phase concurrency and Fourier domain	Retinal vasculature detection, tolerant to noisy retina images
Kovács [156]	2016	Template matching and contour reconstruction	Measurements of vessel's widths, vasculature detection, robust to pathological images
<i>Region-based models</i>			
McInerney [158]	2000	Topology adaptive snakes	Detection of tubular structures, or objects with bifurcations
McInerney [159]	2002	Deformable organism's	Segmentation, labeling, and quantitative analysis of anatomical structures in image
Nain [160]	2004	Region-based active contour model (ACM)	Robust to noisy images, segmentation of tubular structures
Espona [161]	2007	Snakes incorporated with blood vessel topological attributes	Detection of arteriovenous structures in retinal angiographies
Al-Diri [162]	2009	Ribbon of Twin ACM	Computation of retinal vascular segment profiles and vasculature
Sum [164]	2008	Chan–Vese contour model	Extraction of retinal blood vessels
Zhang [165]	2009	Nonlinear orthogonal projection	Localization of retinal vascular network
Faraz [166]	2012	Parabolic modeling	Detection of different stages of retinopathy of prematurity (ROP)
Rouchdy [167]	2013	Geodesic voting approach	Segmentation of complex tree structures in a noisy images, extraction of vessels
Guo [168]	2014	Binary level set based on Mumford–Shah model	Robust to noisy images, vessels extraction
Lermé [169]	2014	Parallel ACM	Robust to normal and pathological images
Zhao [170]	2015	Infinite Perimeter ACM (IPACM)	Analysis of corneal neovascularization
Wang [171]	2015	ACM based on multifeature Gaussian distribution fitting energy	Robust to the image with noises and intensity inhomogeneity
Rad [172]	2016	Morphological region-based initial contour (MRBIC)	Robust to noisy and weak edges of image
Oliveira [173]	2016	Deformable models and the FCM	Extraction of retinal vasculature

The locally normalized concavity measure is suggested to handle the randomly scattered noise in a fundus photograph. These concavity measures are coupled together as indicated by their geometrical properties to extract vessels in fundus photographs.

The physical and functional attributes of double wavelength retinal photographs captured at 570 and 600 nm are used for vessel extraction and classification as arteries and veins [146]. In this method, the dual-Gaussian model

originally utilized in [153] is expanded to approximate the intensity profile of retinal vessels.

A general illustration for ascending and descending physical vessel profiles with variation in the acuity of edges is suggested by Zhu [154]. An input photograph is converted by 24 log-Gabor filters covering six orientations and four scales in symmetric and asymmetric couples. The equality and unevenness of nearby Fourier parts are figured utilizing the scale-invariant trademark and the Kovesi phase

congruency model [155]. The balanced and unbalanced photographs are binaries to get a preliminary segment and a group of edge positions isolating the vessel from non-vessel, respectively, which are further used in an RG procedure for vessel extraction. Kovács and Hajdu [156] proposed a template matching and contour reconstruction for extraction of retinal vessels. It used a generalized Gabor function-based kernels to detect the midlines of vessels. The intensity features of vessel shapes computed in training datasets are remodeled.

Snakes are known as active contour models [157]. A snake is an energy-minimizing spline guided by outward constraint forces and affected by photograph. They lock onto nearby boundaries, localizing them precisely. Several benefits of snakes over traditional attribute extraction approaches are that they are independent and automatic in their finding for a minimal energy state. They can also be simply deployed utilizing outward photograph forces. Snakes are able to trace vibrant elements in temporal as well as the spatial measurements. The key disadvantage of the snakes is that they generally just include boundary data, neglecting other image attributes. Due to this, they often neglect small structures in the procedure of reducing the energy along with the complete route of their contours. Their precision depends on the merging conditions utilized in the energy minimization method; greater precisions need tighter convergence conditions and hence, the greater time complexity. Object tracing, shape identification, segmentation, boundary extraction, and stereo-matching are the major applications of snakes model. The different researchers have inspected the application of active contour models in retinal vessel extraction.

McInerney and Terzopoulos [158] proposed an affine cell image decomposition (ACID) model. The ‘active contour model in ACID’ approach specifically expands traditional snakes, empowering topological flexibility among other attributes. The subsequent topology adaptive snakes are able to fragment some of the most complex-shaped biological features from clinical photographs in an effective and extremely robotic mode. The author has extended the same concept by using ‘deformable organisms’ for automatic vessel extraction, classification and quantitative investigations of physical structures in retina and MR angiograms [159]. Nain et al. [160] presented an implicit deformable model based on image attributes and shape data to develop a region-based active contour that extracts elongated features and penalizes outflows. The approach performed well than the flow based on image statistics only.

Espona et al. [161] utilized the conventional snake along with vessel topological attributes to detect the retinal vascular map. The model is driven by a vessel wrinkle which is really the estimate of vessel midlines distinguished utilizing multilevel set extrinsic curvature based on the structure

tensor. The snake is instated and twisted in view of the outside energy characterized by the vessel wrinkle.

The Ribbon of Twin ACM is proposed for detection of retinal vascular map and vessel width computation in [162]. It utilizes two couples of contours to detect every vessel boundary, while preserving diameter stability. The framework precisely traces the vessel boundaries under challenging situations, light reflex phenomena, consisting of noisy fuzzy boundaries, closely parallel vessels and very fine vessels.

Sum and Cheung suggested an improvement in the Chan and Vese [163] approach by including the local photograph dissimilarity into a level set-based ACM to deal with uneven brightness [164]. The framework is confirmed with trials including both synthetic photographs and medical angiograms.

The nonlinear orthogonal projection-based model is presented to detect the properties of vessel map and develops a new local adaptive thresholding technique for vessel extraction [165]. This framework diverges from existing techniques in that it utilizes MF, vessel tracking, or supervised approaches.

Faraz et al. [166] designed a model for quantification and computation of openness of the major temporal arcade (MTA), including Gabor filters to extract retinal vessels and the Hough transform to identify and parameterize parabolic forms. Observing computations of the openness of the MTA and how they vary over time could assist better analysis and improved medication of retinal abnormalities. The model is tested on the DRIVE dataset.

A novel framework for extraction of vessel map that depends on geodesic voting is proposed by Rouchdy and Cohen [167]. The initial start point is selected manually to extract vessel map with no of any additional information is required. This framework uses fourth dimension or with region-based level sets utilizing shape priors to detect both the midlines and edges of the network. This geodesic voting scheme is tested on different biomedical images, including the DRIVE dataset retinal images to extract vessel map.

Guo et al. [168] designed a retinal vessel detection approach utilizing the Mumford level set that depends on Mumford–Shah model. The matched filter function is used for the blood vessel enhancement followed by the binary level set technique and the Mumford–Shah model to perform segmentation.

The parallel active contour model along with alterations in the presegmentation step is presented for segmentation of retinal vessels in normal and abnormal optics images [169]. However, the presegmentation sometimes becomes inefficient to precisely mark the location of curves near the artery walls.

A novel IPACM with hybrid region forms for the retinal vessel extraction is suggested by Zhao et al. [170]. This

framework takes the benefit of utilizing various kinds of region statistics, e.g., the intensity knowledge and local phase (LP)-based enhancement tree, which is utilized for its dominance in maintaining vessel boundaries while the particular photograph intensity knowledge will assure a precise attribute extraction. This is a first approach which is validated on fluorescein angiography photographs of the VAMPIRE dataset along with other standard DRIVE and STARE datasets.

Wang et al. [171] suggested region-based ACM, which considers picture intensities and ‘vesselness measures’ as two autonomous random variables with various means and variances, and afterward utilizes the two variables to build a multifeature Gaussian distribution fitting energy to enhance the extraction performance of the designed system.

The MRBIC model for vascular extraction of retinal vessel is described by Rad et al. [172]. To avoid any human intervention and drawback of manual setting, statistical and morphological data of the image are used to select an appropriate IC for level set approaches. This model is evaluated on synthetic and real photographs.

In Oliveira et al. [173] approach, the matched filter, and Frangi’s and Gabor Wavelet filter are combined through weighted mean and median ranking and used to enhance

the photographs. The deformable models and the FCM are used for extraction of the retinal vascular network.

The performance evaluation of model-based algorithms for extraction of retinal vessel is shown in Table 20, where the maximum accuracy is stated by Zhang et al. [165] and Kovács and Hajdu [156] on the DRIVE and STARE datasets, respectively.

3.4 Hardware implementation-based approaches

The hardware implementation-based approaches are summarized in Table 21.

Nieto et al. [174] proposed a SIMD design implementation for fast detection of retinal vasculature. It is plotted onto a Spartan 3, amounting to 90 processing elements. The on-chip memory employed was 1.4 MB and saves 8 gray photographs of 144×160 pixels. The operational rate is 53 MHz, sanctioning for a 3×3 convolution in less than 110 μ s. The total time required for segmentation of retinal image having resolution 768×584 is 1.4 s.

A fully automatic framework that depends on the local radon transform and utilizes only techniques that are well parallelizable on GPUs by means of CUDA is presented for extraction of retinal vessels [175]. They allow the evaluation

Table 20 Performance analysis for the model-based techniques

Method	Dataset	Accuracy	Sensitivity	Specificity	AUC
Vermeer [137]	LOCAL	0.9287	0.924	0.921	0.9187
Perfetti [144]	DRIVE	0.9261	–	–	0.9348
Li [145]	DRIVE	–	0.780	0.978	–
	STARE	–	0.752	0.980	–
Lam [147]	STARE	0.9474	–	–	0.9392
Alonso-Montes [148]	DRIVE	0.9185	–	–	0.9011
Lam [152]	DRIVE	0.9472	–	–	0.9614
	STARE	0.9567	–	–	0.9739
Kovács [156]	DRIVE	0.9494	0.7450	0.9793	0.9722
	STARE	0.9610	0.8034	0.9786	0.9836
Espona [161]	DRIVE	0.9316	0.6634	0.9682	–
Al-Diri [162]	DRIVE	–	0.7282	0.9551	–
	STARE	–	0.7521	0.9681	–
Zhang [165]	DRIVE	0.9610	–0.7373	0.9772	–
	STARE	0.9087	–	0.9736	–
Guo [168]	DRIVE	0.9512	0.784	0.980	–
	STARE	0.9521	0.753	0.981	–
Zhao [165]	DRIVE	0.954	0.742	0.982	0.862
	STARE	0.956	0.780	0.978	0.874
	VAMPIRE	0.977	0.729	0.985	0.857
Wang [171]	STARE	0.944	0.758	0.965	0.862
Rad [172]	DRIVE	0.9608	0.6965	0.9722	–
	STARE	0.9289	0.7342	0.9608	–
Oliveira [173]	DRIVE	0.9464	0.8644	–	0.9513
	STARE	0.9532	0.8254	–	0.9544

Table 21 Summarization of hardware implementation-based retinal vessel segmentation methods

References	Year	Techniques	Results for medical examination and applications
Nieto [174]	2009	FPGA implementation with SIMD	Real-time retinal vascular tree detection
Krause [175]	2013	CUDA-based implementation on general-purpose graphics processing units (GPUs)	High-speed extraction of retinal vessels
Koukounis [176]	2014	FPGA-based implementation, MFR, thresholding	Low-power, real-time retinal vasculature extraction
Argüello [177]	2014	CUDA-based implementation on GPUs	Extraction of the retinal vascular network

of huge datasets in a short time span. Preprocessing steps consist of a black top hat pursued by a Gaussian convolution. It is possible to process photographs of resolution 4288×2848 pixels in 1.2 s on an NVIDIA Geforce GTX680. The DRIVE dataset is used for performance evaluation of this approach. Its disadvantage is the high power consumption (the GPU platform requires approximately 500 W) to execute the segmentation operation, which is not acceptable in embedded applications.

Koukounis et al. [176] suggested a VLSI implementation for extraction of retinal vascular tree while analyzing different attributes that affect the power utilization, precision and efficiency of the framework. This is an unsupervised approach which uses MF with signed integers to increase the variance between the vessel and background pixels. The system speeds up the operation of attaining a binary vessels map by utilizing parallel processing and efficient resource sharing, achieving real-time performance. The system is tested on a commercial FPGA design and shows distinct performance enhancements when contested with current similar techniques. Additionally, the low power requirement of this design permits the suggested design to be utilized in portable frameworks, as it attains an efficient stability between execution, power utilization, and precision.

Another approach is modified from [176] and completely redefined to be implemented in CUDA-based GPUs [177]. This approach is assembled in a PC platform containing a four-core Intel Core i7 860 CPU with 8 GB of RAM, utilizing a 64-bit Linux GNU compiler and CUDA 5.0 with the -O3 and -sm_20 flags. This method is based on filtering and contour tracking algorithms. This algorithm contains five major steps: a quick approximation of the retinal vessel map and four steps related to contour tracing based on ACM and a final postprocessing step.

Figure 5 summarizes the performance measures for hardware-based implementation techniques of retinal vessel extraction, where the maximum accuracy is obtained by Krause et al. [175] and Argüello et al. [177] on the DRIVE and STARE datasets, correspondingly.

3.5 Hybrid approaches

Table 22 summarizes the hybrid methods, which use multiple techniques or classifiers for extraction of retinal vessels.

Villalobos-Castaldi et al. [178] introduced a technique that depends on the second local entropy and on the GLCM for extraction of retinal vasculature. The most important factor is the thresholding value. This approach provides a powerful tool to acquire an automatic threshold limit to extract the vessel and relies upon only on the knowledge enclosed in the evaluated photograph. The DRIVE dataset is used for the evaluation of this approach.

A model of hysteresis-classifier scheme for detection of retinal vascular map is used in [179]. It consists of two classifiers: The first one, called the pessimist, works with a practically zero FPR, which with overlapping classes indicates a high false-negative rate (FNR); the second one, called the optimist, works with a practically zero FNR and a high FPR. Then, utilizing the preceding information about the connectivity characteristic of vessels, the pessimist sorting can be utilized to choose true vessels from among the optimist sorting.

Mudassar and Saira [180] suggested a combination of four different techniques; ILCS, EEED, MMF, and CA for extraction of retinal vessels. ILCS, EEED, and CA are new additions, whereas MMF is an enhanced and improved version of the current MF approach. CA is a favorable method.

Saleh Shahbeig [181] presented a fast and automatic morphological-based retinal vessel segmentation system utilizing CT and PCA. CT is utilized to improve the contrast of retinal photographs by making prominent the boundary of photographs in different measures and orientations. An enhanced morphology procedure with multidirectional structure components is utilized to detect the retinal vessel network. CCA and an adaptive filter are utilized to refine appeared frills with the size of smaller than arterioles in photographs.

A combination of HCF with a discriminative learning system is proposed in [1]. The SWT and WLD both extract the curvilinear structures. The Gabor responses and vesselness filter are used for vessel detection. The new vessel attributes as well as conventional filter-based attributes segmented

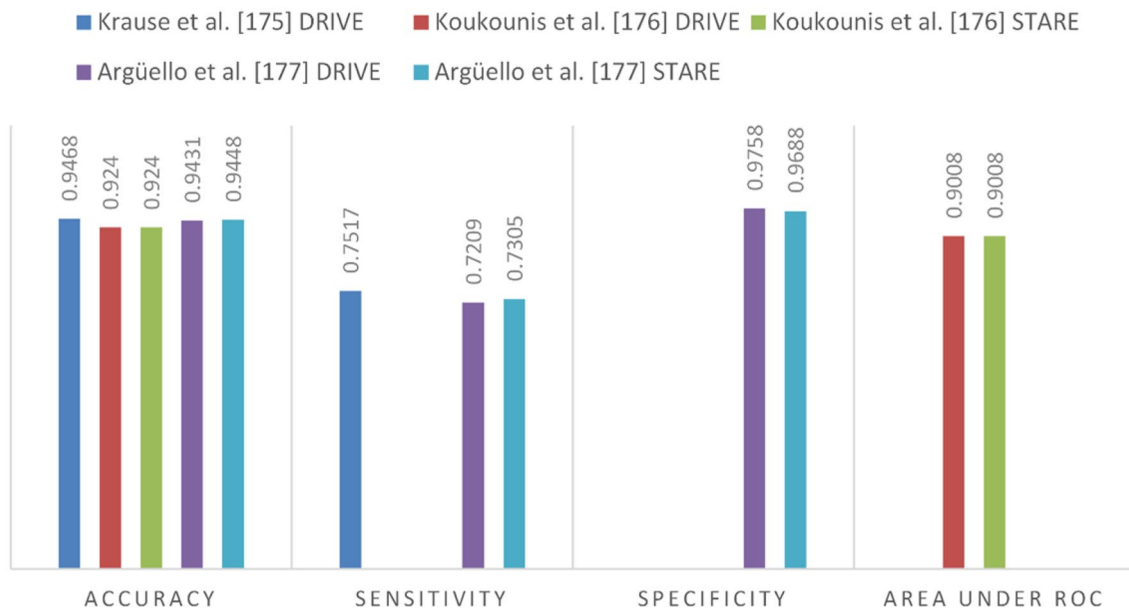


Fig. 5 Performance metrics for hardware implementation-based approaches

Table 22 Summarization of hybrid approaches for retinal vessel segmentation

References	Year	Techniques	Results for medical examination and applications
Villalobos [178]	2010	Second local entropy, GLCM, MF	Detection of retinal vascular map
Condurache [179]	2012	Hysteresis binary-classification paradigm, pessimist and optimist classifiers	Tolerant to both normal and pathological images, extraction of retinal vessels
Mudassar [180]	2013	Image line cross-sections (ILCS), edge enhancement and edge detection (EEED), modified matched filtering (MMF), and continuation algorithm (CA)	Localization of vascular network of pathological retina images
Saleh Shahbeig [198]	2013	Curvelet transform (CT) and principle component analysis (PCA), multidirectional morphology functions, connected component analysis (CCA)	Robust to noisy and normal retinal images for vasculature extraction
Cheng [1]	2014	Stroke width transform (SWT) and Weber’s local descriptors (WLD), Gabor responses and vesselness measurements, random forest (RF), hybrid context-aware features (HCF)	Suitable for localization of blood vessels in normal and pathological retina images
Salazar-Gonzalez [181]	2014	Markov random field (MRF) and compensation factor into the graph cut approach, CLAHE, binary opening and distance transform	Robust to normal and pathological retinal images for vascular network detection
Jiang [182]	2015	Isotropic undecimated wavelet transform (IUWT), texture entropy, and FCM classifier	Fast extraction of blood vessels from normal and pathological retina images
Dai [183]	2015	Gray-voting approach, 2-D Gabor filter, GMM classifier	Segmentation of retinal vessels network

from orientation invariant local context are used as an input into an RF approach for pixel level vessel segmentation.

Salazar-Gonzalez et al. [181] introduced a graph cut method for detection of retinal vascular tree. Two different approaches, MRF image reconstruction technique and compensation factor scheme are evaluated in this article for detection of retinal vessels and OD.

A combination of IUWT, texture entropy, and FCM classifier is proposed in [182]. IUWT is used on the pre-processed photograph to denoise the retinal photograph in its frequency field. FCM on texture attributes based on local gray value entropy is used to extract retinal vessel network.

Dai et al. [183] proposed a gray-voting approach for segmentation of retinal vasculature. The gray-voting technique

is utilized to improve the contrast of tiny vessels, while a 2-D Gabor wavelet is applied to segment the major vessels. The gray-voting outcomes are fused with the 2-D Gabor filter outcomes as preprocessing result. A GMM classifier is then applied to detect vessel segments from the preprocessing result, while tiny vessel segments are acquired utilizing another gray-voting procedure, which counterparts the vessel segment detection previously used.

The performance metrics for hybrid approaches of retinal vessel extraction is shown in Table 23, where the highest accuracy is attained by Villalobos-Castaldi et al. [178] and Cheng et al. [1] on the DRIVE and STARE datasets, respectively.

4 Discussion and conclusion

It is observed that the DRIVE and STARE databases are mostly utilized for validation of different retinal vessel extraction algorithms. Figure 6 displays the frequency of the distribution of datasets used by different retinal segmentation techniques.

The supervised approaches show better performance than unsupervised approaches. However, the performance of supervised techniques reduces on the photographs with uneven brightness because of the increase in FPR in some photographs on the boundary of the OD, hemorrhages, and other kinds of disorders that exist in prominent contrast. The automatic vessel extraction of fundus images has been performed by utilizing MF. Various enhancements and adaptations techniques are suggested based on Gaussian MF by Chaudhuri et al. [64]. The MF alone cannot deal with the extraction of vessel in abnormal fundus photographs; therefore it is usually coupled with other techniques [71, 75]. The issue of the central vessel reflex is addressed by coupling the Gaussian model [142, 146] with ACM [162]. The Sofka and Stewart handle the issue of overlying of the background

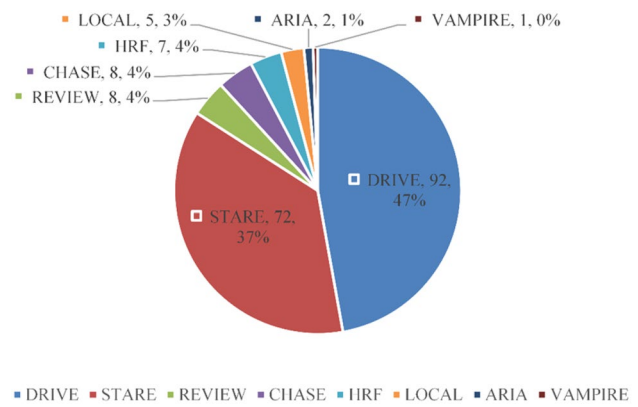


Fig. 6 The frequency of the distribution of datasets

structures like the retinal edge and the OD in the vascular map detection [25]. The multi-concavity modeling [152] and the DVFs [147] are very effective in handling various retinal abnormalities. The union of radial projections with steerable wavelets and semi-supervised arrangement [184] produced efficient results in the extraction of tiny and poor resolution vessels, thus showing maximum sensitivity. The Gabor filters are very helpful in fundus photograph evaluation. Moreover, along with vessel extraction [86, 88] the Gabor wavelet transform has also been used for the robust fractal exploration of the retinal vascular map.

It is noticed that few articles express the performance in terms of accuracy and AUC, whereas the other papers select sensitivity and specificity for evaluating the performance. The methodology having the highest accuracy of each category on the DRIVE and STARE databases is depicted in Figs. 7 and 8, correspondingly. The highest AUC of each category of the both databases is represented in Figs. 9 and 10, correspondingly.

Accurate detection of retinal veins is a fundamental step in computer-assisted diagnostic (CAD) analysis and medical

Table 23 Performance metrics for hybrid methods

Method	Dataset	Accuracy	Sensitivity	Specificity	AUC
Villalobos-Castaldi et al. [178]	DRIVE	0.9759	0.9648	0.9480	–
Condurache and Mertins [179]	DRIVE	0.9516	0.9094	0.9591	0.9726
	STARE	0.9595	0.8902	0.9673	0.9791
Saleh Shahbeig [198]	DRIVE	0.9458	0.7612	–	–
	CHENG et al. [1]	DRIVE	0.9474	0.7252	0.9798
CHENG et al. [1]	STARE	0.9633	0.7813	0.9843	0.9844
	HRF	0.9647	0.7889	0.9865	–
	Salazar-Gonzalez et al. [181]	DRIVE	0.9412	0.7512	–
STARE		0.9441	0.7887	–	–
Jiang et al. [182]	DRIVE	–	0.8205	–	0.9375
Dai et al. [183]	DRIVE	0.9418	0.7359	0.9720	–
	STARE	0.9364	0.7769	0.9550	–

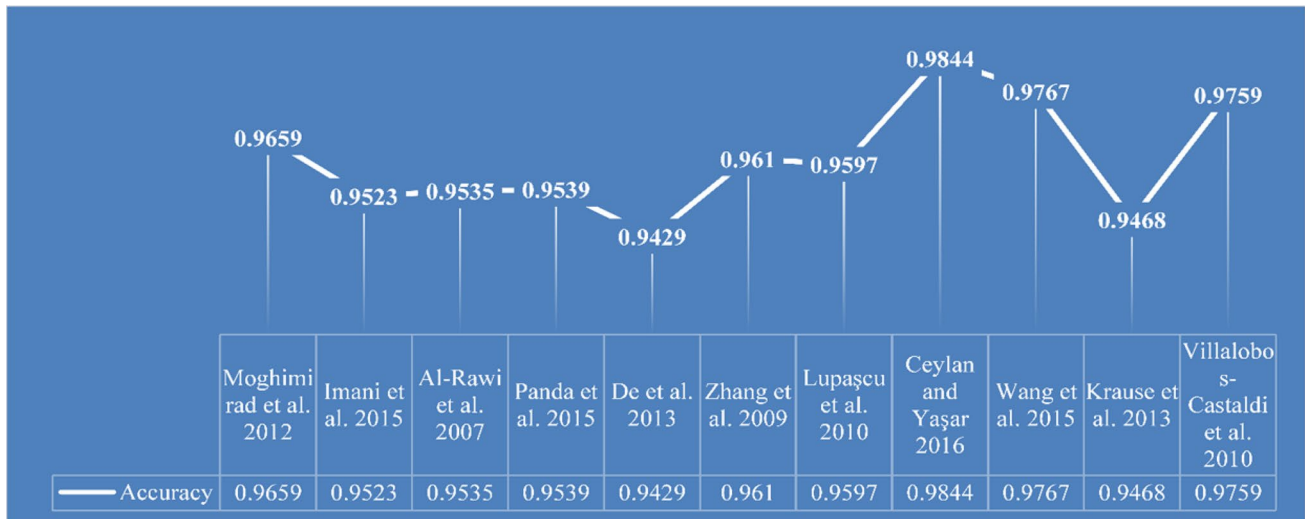


Fig. 7 Highest accuracy of the each category on the DRIVE dataset

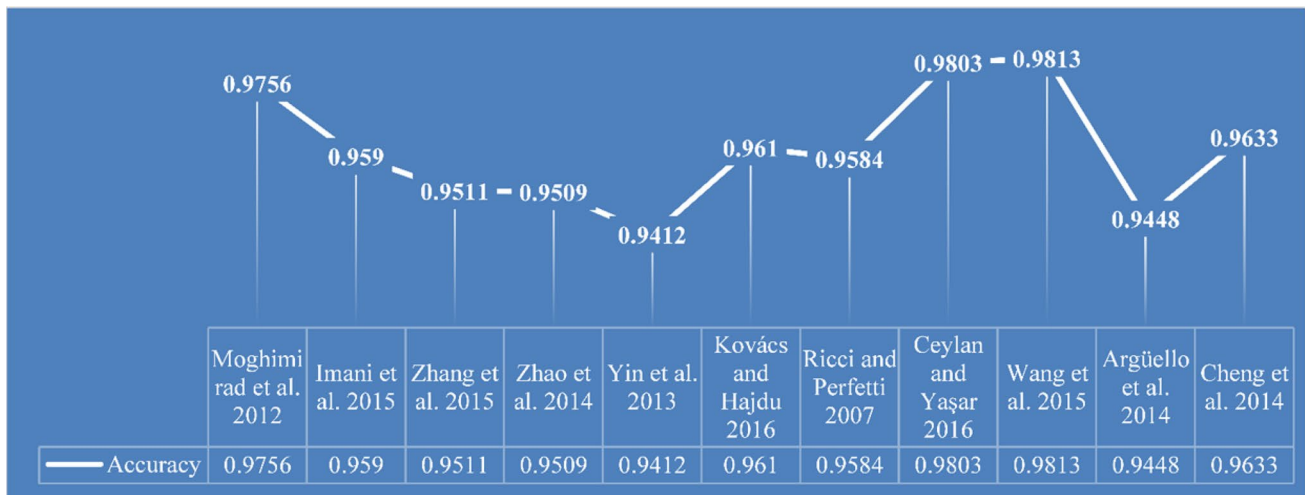


Fig. 8 Highest accuracy of the each category on the STARE dataset

screening of retinopathy. Although high quality of fundus images is available, isolation of the veins and retinal background is still a challenging task. Moreover, pathological disorders of the retinal vessel structure can be seen in various ailments, such as diabetes, hypertension, stroke, and glaucoma. Despite the development of different promising supervised and unsupervised techniques, there is still room for improvement. Table 2, summarizes algorithms developed for extraction of retinal vasculature till now. Some of the reviewed techniques handle both healthy and unhealthy retinal images. Some of those are appropriate for investigation of noisy and central reflex images. Most of the published articles are validated on a limited range of databases which contain a small number of photographs. The performance

metrics showed in a large portion of the articles are computed on a limited number of photographs of specific morphological attributes. The limited number of photographs in the DRIVE and STARE datasets do not accommodate for the image-associated attributes, for example inter-image and intra-image variation in luminance, uneven contrast and non-uniform background gray-level qualities. The expansion of approaches, valid for photographs obtained from various imaging system, under diverse environmental situations is also an open range for exploration of vessel extraction methodologies.

Vessel extraction is the fundamental step for abnormality detection. There are large volume of photographs obtained from different kinds of fundus camera. Furthermore, the vast

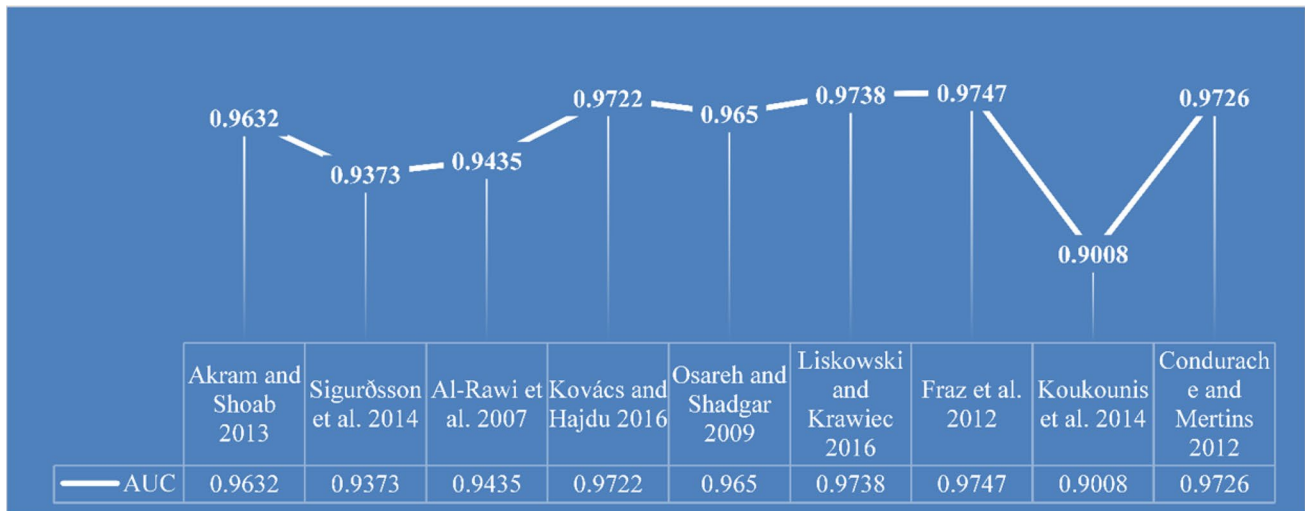


Fig. 9 Highest AUC of the each category on the DRIVE dataset

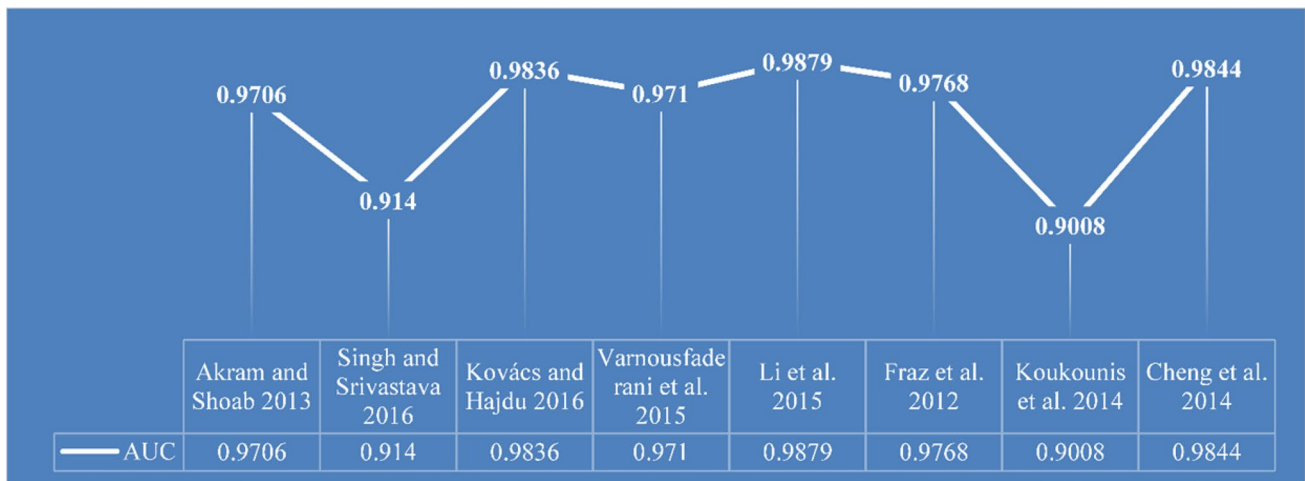


Fig. 10 Highest AUC of the each category on the STARE dataset

majority of the published techniques are validated on the limited number databases, i.e., DRIVE and STARE. The quality of photographs from these databases is constrained to 0.4 and 0.3 megapixels, correspondingly. This poor contrast is satisfactory for specific considerations like fractal dimension or tortuosity, and computing the vessel width usually needs greater resolution photographs to attain superior accuracy. An advancement in image acquisition brings it easy to collect a large number of patient photographs for analysis. Analysis of these photographs needs fast detection techniques strong enough to execute the photographs obtained from different image capture equipments and imaging conditions. The hardware-based implementations approaches suggest a solution providing high processing speed that is essential in real-time applications.

For accurate and efficient CAD system, precision and strength of the extraction method are important. This article offers an extensive report of existing retinal vessel extraction techniques. We have enclosed both initial and latest articles concentrating on extraction of retinal vasculature methodologies and approaches. Our objective is to present the existing extraction methods, provide the reader an outline for the current research, and to recommend the array of retinal vessel extraction techniques found in the literature. The present drifts, the future guidelines, and the open hitches in the automated retinal vessel extraction are also debated.

Compliance with ethical standards

Conflict of interest The authors declare that they have no conflict of interest.

References

1. Cheng E, Du L, Wu Y, Zhu Y, Megalooikonomou V, Ling H (2014) Discriminative vessel segmentation in retinal images by fusing context-aware hybrid features. *Mach Vis Appl* 25(7):1779–1792
2. Abramoff M, Garvin M, Sonka M (2010) Retinal imaging and image analysis. *IEEE Rev Biomed Eng* 3:169–208
3. Jelinek H, Cree M (2009) Automated image detection of retinal pathology. CRC Press, Boca Raton
4. Patton N, Aslam T, MacGillivray T, Deary I, Dhillon B, Eikelboom R, Yogesani K, Constable I (2006) Retinal image analysis: concepts, applications and potential. *Prog Retin Eye Res* 25(1):99–127
5. Franklin S, Rajan S (2014) Computerized screening of diabetic retinopathy employing blood vessel segmentation in retinal images. *Biocybern Biomed Eng* 34(2):117–124
6. Fraz M, Remagnino P, Hoppe A, Uyyanonvara B, Rudnicka A, Owen C, Barman S (2012) Blood vessel segmentation methodologies in retinal images—a survey. *Comput Methods Programs Biomed* 108(1):407–433
7. Jusoh F, Haron H, Ibrahim R, Azemin M (2016) An overview of retinal blood vessels segmentation. *Advanced computer and communication engineering technology*. Springer, Berlin, pp 63–71
8. GeethaRamani R, Balasubramanian L (2016) Retinal blood vessel segmentation employing image processing and data mining techniques for computerized retinal image analysis. *Biocybern Biomed Eng* 36(1):102–118
9. Garhöfer G, Vilser W (2012) Measurement of retinal vessel diameters. *Ocular blood flow*. Springer, Berlin, pp 101–122
10. Niemeijer M, Staal J, Ginneken BV, Loog M, Abramoff M (2004) Comparative study of retinal vessel segmentation methods on a new publicly available database. In: *Medical imaging. International society for optics and photonics*, pp 648–656
11. Dai P, Luo H, Sheng H, Zhao Y, Li L, Wu J, Zhao Y, Suzuki K (2015) A new approach to segment both main and peripheral retinal vessels based on gray-voting and Gaussian mixture model. *PLoS ONE* 10(6):e0127748
12. Mabrouk M, Solouma N, Kadah Y (2006) Survey of retinal image segmentation and registration. *GVIP J* 6(2):1–11
13. Winder R, Morrow P, McRitchie I, Bailie J, Hart P (2009) Algorithms for digital image processing in diabetic retinopathy. *Comput Med Imaging Graph* 33(8):608–622
14. Faust O, Acharya R, Ng E, Ng K, Suri J (2012) Algorithms for the automated detection of diabetic retinopathy using digital fundus images: a review. *J Med Syst* 36(1):145–157
15. WHO Organization (2016) Global report on diabetes. In: *WHO Library Cataloguing-in-Publication Data*. http://apps.who.int/iris/bitstream/10665/204871/1/9789241565257_eng.pdf
16. Alberti K, Zimmet P (1998) Definition, diagnosis and classification of diabetes mellitus and its complications. Part 1: diagnosis and classification of diabetes mellitus, Provisional report of a WHO consultation. *Diabet Med* 15(7):539–553
17. Reaven G (1998) Role of insulin resistance in human disease. *Diabetes* 37(12):1595–1607
18. Ong G, Ripley L, Newsom R, Cooper M, Casswell A (2004) Screening for sight-threatening diabetic retinopathy: comparison of fundus photography with automated color contrast threshold test. *Am J Ophthalmol* 137(3):445–452
19. Tielsch J, Katz J, Singh K, Quigley H, Gottsch J, Javitt J, Sommer A (1991) A population-based evaluation of glaucoma screening: the Baltimore eye survey. *Am J Epidemiol* 134(10):1102–1110
20. Heijl A, Leske M, Bengtsson B, Hyman L, Bengtsson B, Hussein M (2002) Reduction of intraocular pressure and glaucoma progression: results from the early manifest glaucoma trial. *Arch Ophthalmol* 120(10):1268–1279
21. Brothers RHL, King W, Clegg L, Klein R, Cooper L, Sharrett A, Davis M, Cai J (1999) Atherosclerosis risk in communities study group. methods for evaluation of retinal microvascular abnormalities associated with hypertension/sclerosis in the atherosclerosis risk in communities study. *Ophthalmology* 106(12):2269–2280
22. Lim L, Mitchell P, Seddon J, Holz F, Wong T (2012) Age-related macular degeneration. *The Lancet* 379(9827):1728–1738
23. Wong C, Yanagi Y, Lee W, Ogura Y, Yeo I, Wong T, Cheung C (2016) Age-related macular degeneration and polypoidal choroidal vasculopathy in Asians. *Prog Retinal Eye Res* 53:107–139
24. Frangi A, Niessen W, Vincken K, Viergever M (1998) Multiscale vessel enhancement filtering. In: *Medical image computing and computer-assisted intervention—MICCAI'98*. Springer, Berlin Heidelberg, pp 130–137
25. Sofka M, Stewart C (2006) Retinal vessel centerline extraction using multiscale matched filters, confidence and edge measures. *IEEE Trans Med Imaging* 25(12):1531–1546
26. Hoover A, Kouznetsova V, Goldbaum M (2000) Locating blood vessels in retinal images by piece-wise threshold probing of a matched filter response. *IEEE Trans Med Imaging* 19(3):203–210
27. Martínez-Pérez M, Hughes A, Stanton A, Thom S, Bharath A, Parker K (1999) Retinal blood vessel segmentation by means of scale-space analysis and region growing. In: *medical image computing and computer-assisted intervention—MICCAI'99*. Springer, Berlin Heidelberg, pp 90–97
28. Martínez-Pérez M, Hughes A, Thom S, Bharath A, Parker K (2007) Segmentation of blood vessels from red-free and fluorescein retinal images. *Med Image Anal* 11(1):47–61
29. Farnell D, Hatfield F, Knox P, Reakes M, Spencer S, Parry D, Harding S (2008) Enhancement of blood vessels in digital fundus photographs via the application of multiscale line operators. *J Frankl Inst* 345(7):748–765
30. Vlachos M, Dermatas E (2010) Multi-scale retinal vessel segmentation using line tracking. *Comput Med Imaging Graph* 34(3):213–227
31. Li Q, You J, Zhang D (2012) Vessel segmentation and width estimation in retinal images using multiscale production of matched filter responses. *Expert Syst Appl* 39(9):7600–7610
32. Moghimirad E, Rezaatfighi S, Soltanian-Zadeh H (2012) Retinal vessel segmentation using a multi-scale medialness function. *Comput Biol Med* 42(1):50–60
33. Yu H, Barriga S, Agurto C, Zamora G, Bauman W, Soliz P (2012) Fast vessel segmentation in retinal images using multiscale enhancement and second-order local entropy. In: *SPIE medical imaging. International society for optics and photonics*, pp 83151B–83151B
34. Ricci E, Perfetti R (2007) Retinal blood vessel segmentation using line operators and support vector classification. *IEEE Trans Med Imaging* 26(10):1357–1365
35. Nguyen U, Bhuiyan A, Park L, Ramamohanarao K (2013) An effective retinal blood vessel segmentation method using multi-scale line detection. *Pattern Recognit* 46(3):703–715
36. Fathi A, Naghsh-Nilchi A (2013) Automatic wavelet-based retinal blood vessels segmentation and vessel diameter estimation. *Biomed Signal Process Control* 8(1):71–80
37. Azzopardi G, Petkov N (2013) Trainable COSFIRE filters for keypoint detection and pattern recognition. *IEEE Trans Pattern Anal Mach Intell* 35(2):490–503
38. Akram M, Khan S (2013) Multilayered thresholding-based blood vessel segmentation for screening of diabetic retinopathy. *Eng Comput* 29(2):165–173
39. Wang Y, Ji G, Lin P, Trucco E (2013) Retinal vessel segmentation using multiwavelet kernels and multiscale hierarchical decomposition. *Pattern Recognit* 46(8):2117–2133

40. Ganjee R, Azmi R, Gholizadeh B (2014) An improved retinal vessel segmentation method based on high level features for pathological images. *J Med Syst* 38(9):1–9
41. Zhang B, Zhang L, Zhang L, Karray F (2010) Retinal vessel extraction by matched filter with first-order derivative of Gaussian. *Comput Biol Med* 40(4):438–445
42. Mapayi T, Viriri S, Tapamo J (2014) A new adaptive thresholding technique for retinal vessel segmentation based on local homogeneity information. In: *Image and signal processing*. Springer, pp 558–567
43. Ravichandran C, Raja J (2014) A fast enhancement/thresholding based blood vessel segmentation for retinal image using contrast limited adaptive histogram equalization. *J Med Imaging Health Inf* 4(4):567–575
44. Annunziata R, Garzelli A, Ballerini L, Mecocci A, Trucco E (2015) Leveraging multiscale hessian-based enhancement with a novel exudate inpainting technique for retinal vessel segmentation. *IEEE J Biomed Health Inf* 20(4):1129–1138
45. Marin D, Aquino A, Gegundez-Arias M, Bravo J (2011) A new supervised method for blood vessel segmentation in retinal images by using gray-level and moment invariants-based features. *IEEE Trans Med Imaging* 30:146–158
46. Fraz M, Welikala R, Rudnicka A, Owen C, Strachan D, Barman S (2015) QUARTZ: quantitative analysis of retinal vessel topology and size—an automated system for quantification of retinal vessels morphology. *Expert Syst Appl* 42(20):7221–7234
47. Bao XR, Ge X, She LH, Zhang S (2015) Segmentation of retinal blood vessels based on cake filter. *BioMed Res Int* 2015:137024–137024
48. Kar S, Maity S (2016) Blood vessel extraction and optic disc removal using curvelet transform and kernel fuzzy c-means. *Comput Biol Med* 70:174–189
49. Emary E, Zawbaa H, Hassanien A, Parv B (2016) Multi-objective retinal vessel localization using flower pollination search algorithm with pattern search. *Adv Data Anal Classif* 11:1–7
50. Shehhi RA, Marpu P, Woon W (2016) An automatic cognitive graph-based segmentation for detection of blood vessels in retinal images. *Mathe Probl Eng* 2016:15. <https://doi.org/10.1155/2016/7906165>
51. Khan KB, Khaliq AA, Shahid M (2016) A morphological hessian based approach for retinal blood vessels segmentation and denoising using region based otsu thresholding. *PLoS ONE* 11(7):e0158996
52. Mendonca A, Campilho A (2006) Segmentation of retinal blood vessels by combining the detection of centerlines and morphological reconstruction. *IEEE Trans Med Imaging* 25(9):1200–1213
53. Zana F, Jean-Claude K (2001) Segmentation of vessel-like patterns using mathematical morphology and curvature evaluation. *IEEE Trans Image Process* 10(7):1010–1019
54. Ayala G, León T, Zapater V (2005) Different averages of a fuzzy set with an application to vessel segmentation. *IEEE Trans Fuzzy Syst* 13(3):384–393
55. Yang Y, Huang S, Rao N (2008) An automatic hybrid method for retinal blood vessel extraction. *Int J Appl Math Comput Sci* 18(3):399–407
56. Fraz M, Remagnino P, Hoppe A, Uyyanonvara B, Owen C, Rudnicka A, Barman S (2011) Retinal vessel extraction using first-order derivative of Gaussian and morphological processing. In: *Advances in visual computing*. Springer, Berlin Heidelberg, pp 410–420
57. Miri M, Mahloojifar A (2011) Retinal image analysis using curvelet transform and multistructure elements morphology by reconstruction. *IEEE Trans Biomed Eng* 58(5):1183–1192
58. Rossant F, Badellino M, Chavillon A, Bloch I, Paques M (2011) A morphological approach for vessel segmentation in eye fundus images, with quantitative evaluation. *J Med Imaging Health Inf* 1(1):42–49
59. Fraz M, Barman S, Remagnino P, Hoppe A, Basit A, Uyyanonvara B, Rudnicka A, Owen C (2012) An approach to localize the retinal blood vessels using bit planes and centerline detection. *Comput Methods Programs Biomed* 108(2):600–616
60. Fraz M, Basit A, Barman S (2013) Application of morphological bit planes in retinal blood vessel extraction. *J Digit Imaging* 26(2):274–286
61. Xu Y, Géraud T, Najman L (2013) Two applications of shape-based morphology: blood vessels segmentation and a generalization of constrained connectivity. In: *Mathematical morphology and its applications to signal and image processing*. Springer, Berlin Heidelberg, pp 390–401
62. Sigurðsson E, Valero S, Benediktsson J, Chansussot J, Talbot H, Stefánsson E (2014) Automatic retinal vessel extraction based on directional mathematical morphology and fuzzy classification. *Pattern Recognit Lett* 47:164–171
63. Imani E, Javidi M, Pourreza H (2015) Improvement of retinal blood vessel detection using morphological component analysis. *Comput Methods Programs Biomed* 118(3):263–279
64. Chaudhuri S, Chatterjee S, Katz N, Nelson M, Goldbaum M (1989) Detection of blood vessels in retinal images using two-dimensional matched filters. *IEEE Trans Med Imaging* 8(3):263–269
65. Zhou L, Rzeszutarski M, Singerman L, Chokreff J (1994) The detection and quantification of retinopathy using digital angiograms. *IEEE Trans Med Imaging* 13(4):619–626
66. Al-Rawi M, Qutaishat M, Arrar M (2007) An improved matched filter for blood vessel detection of digital retinal images. *Comput Biol Med* 37(2):262–267
67. Zhang L, Li Q, You J, Zhang D (2009) A modified matched filter with double-sided thresholding for screening proliferative diabetic retinopathy. *IEEE Trans Inf Technol Biomed* 13(4):528–534
68. Gang L, Chutatape O, Krishnan SM (2002) Detection and measurement of retinal vessels in fundus images using amplitude modified second-order Gaussian filter. *IEEE Trans Biomed Eng* 49(2):168–172
69. Jiang X, Mojon D (2003) Adaptive local thresholding by verification-based multithreshold probing with application to vessel detection in retinal images. *IEEE Trans Pattern Anal Mach Intell* 25(1):131–137
70. Sukkaew L, Uyyanonvara B, Barman S, Fielder A, Cocker K (2007) Automatic extraction of the structure of the retinal blood vessel network of premature infants. *J Med Assoc Thai* 90(9):1780–1792
71. Cinsdikici M, Aydın D (2009) Detection of blood vessels in ophthalmoscope images using MF/ant (matched filter/ant colony) algorithm. *Comput Methods Programs Biomed* 96(2):85–95
72. Amin M, Yan H (2011) High speed detection of retinal blood vessels in fundus image using phase congruency. *Soft Comput* 15(6):1217–1230
73. Kaba D, Salazar-Gonzalez A, Li Y, Liu X, Serag A (2013) Segmentation of retinal blood vessels using gaussian mixture models and expectation maximisation. In: *Health Information Science*. Springer, Berlin Heidelberg, pp 105–112
74. Chakraborti T, Jha D, Chowdhury A, Jiang X (2015) A self-adaptive matched filter for retinal blood vessel detection. *Mach Vis Appl* 26(1):55–68
75. Zhang J, Bekkers E, Abbasi S, Dashtbozorg B, Romeny BTH (2015) Robust and fast vessel segmentation via Gaussian derivatives in orientation scores. In: *Image analysis and processing—ICIAP 2015*. Springer, pp 537–547

76. Singh N, Srivastava R (2016) Retinal blood vessels segmentation by using Gumbel probability distribution function based matched filter. *Comput Methods Programs Biomed* 129:40–50
77. Fadzil MA, Izhar L, Venkatachalam P, Karunakar T (2007) Extraction and reconstruction of retinal vasculature. *J Med Eng Technol* 31(6):435–442
78. Palomera-Pérez M, Martínez-Pérez M, Benítez-Pérez H, Ortega-Arjona J (2010) Parallel multiscale feature extraction and region growing: application in retinal blood vessel detection. *IEEE Trans Inf Technol Biomed* 14(2):500–506
79. Jiang H, He B, Fang D, Ma Z, Yang B, Zhang L (2013). A region growing vessel segmentation algorithm based on spectrum information. *Comput Math Methods Med* 2013:743870–743870
80. Zhao Y, Wang X, Wang X, Shih F (2014) Retinal vessels segmentation based on level set and region growing. *Pattern Recognit* 47(7):2437–2446
81. Dizdaroğlu B, Ataer-Cansizoglu E, Kalpathy-Cramer J, Keck K, Chiang M, Erdogmus D (2014) Structure-based level set method for automatic retinal vasculature segmentation. *EURASIP J Image Video Process* 2014(1):1–26
82. You S, Bas E, Erdogmus D, Kalpathy-Cramer J (2011) Principal curved based retinal vessel segmentation towards diagnosis of retinal diseases. In: *Healthcare informatics, imaging and systems biology (HISB), 2011 first IEEE international conference*. IEEE, pp 331–337
83. Panda R, Puhan NB, Panda G (2016). New binary Hausdorff symmetry measure based seeded region growing for retinal vessel segmentation. *Biocybern Biomed Eng* 36(1):119–129
84. Lázár I, Hajdu A (2015) Segmentation of retinal vessels by means of directional response vector similarity and region growing. *Comput Biol Med* 66:209–221
85. Staal J, Abràmoff M, Niemeijer M, Viergever M, Ginneken BV (2004) Ridge-based vessel segmentation in color images of the retina. *IEEE Trans Med Imaging* 23(4):501–509
86. Soares J, Leandro J, Jr RC, Jelinek H, Cree M (2006) Retinal vessel segmentation using the 2-D Gabor wavelet and supervised classification. *IEEE Trans Med Imaging* 25(9):1214–1222
87. Anzalone A, Bizzarri F, Parodi M, Storace M (2008) A modular supervised algorithm for vessel segmentation in red-free retinal images. *Comput Biol Med* 38(8):913–922
88. Osareh A, Shadgar B (2009) Automatic blood vessel segmentation in color images of retina. *Iran J Sci Technol* 33(B2):191–206
89. Xu L, Luo S (2010) A novel method for blood vessel detection from retinal images. *Biomed Eng Online* 9(1):14
90. Lupaşcu C, Tegolo D, Trucco E (2010) FABC: retinal vessel segmentation using AdaBoost. *IEEE Trans Inf Technol Biomed* 14(5):1267–1274
91. You X, Peng Q, Yuan Y, Cheung Y, Lei J (2011) Segmentation of retinal blood vessels using the radial projection and semi-supervised approach. *Pattern Recognit* 44(10):2314–2324
92. Varnousfaderani E, Yousefi S, Bowd C, Belghith A, Goldbaum M (2015) Vessel delineation in retinal images using leung-malik filters and two levels hierarchical learning. *AMIA Annu Symp Proc* 2015:1140 **American Medical Informatics Association**
93. Roychowdhury S, Koozekanani D, Parhi K (2015) Blood vessel segmentation of fundus images by major vessel extraction and subimage classification. *IEEE J Biomed Health Inf* 19(3):1118–1128
94. Orlando JI, Prokofyeva E, Blaschko MB (2017) A discriminatively trained fully connected conditional random field model for blood vessel segmentation in fundus images. *IEEE Trans Biomed Eng* 64(1):16–27
95. Akita K, Kuga H (1982) A computer method of understanding ocular fundus images. *Pattern Recognit* 15(6):431–443
96. Sinthanayothin C, Boyce J, Cook H, Williamson T (1999) Automated localization of the optic disc, fovea, and retinal blood vessels from digital color fundus images. *Br J Ophthalmol* 83(8):902–910
97. Nekovei R, Sun Y (1995) Back-propagation network and its configuration for blood vessel detection in angiograms. *IEEE Trans Neural Netw* 6(1):64–72
98. Yao C, Chen H (2009) Automated retinal blood vessels segmentation based on simplified PCNN and fast 2D-Otsu algorithm. *J Cent South Univ Technol* 16:640–646
99. Lupaşcu C, Tegolo D (2010) Automatic unsupervised segmentation of retinal vessels using self-organizing maps and k-means clustering. In: *Computational intelligence methods for bioinformatics and biostatistics*. Springer, Berlin Heidelberg, pp 263–274
100. Vega R, Guevara E, Falcon L, Sanchez-Ante G, Sossa H (2013) Blood vessel segmentation in retinal images using lattice neural networks. In: *Advances in artificial intelligence and its applications*. Springer, Berlin Heidelberg, pp 532–544
101. Vega R, Sanchez-Ante G, Falcon-Morales L, Sossa H, Guevara E (2015) Retinal vessel extraction using lattice neural networks with dendritic processing. *Comput Biol Med* 58:20–30
102. Sossa H, Guevara E (2014) Efficient training for dendrite morphological neural networks. *Neurocomputing* 131:132–142
103. Andersson T, Lathen G, Lenz R, Borga M (2013) Modified gradient search for level set based image segmentation. *IEEE Trans Image Process* 22(2):621–630
104. Anitha J, Hemanth D (2013) An efficient Kohonen-fuzzy neural network based abnormal retinal image classification system. *Neural Netw World* 23(2):149–167
105. Franklin S, Rajan S (2014) Retinal vessel segmentation employing ANN technique by Gabor and moment invariants-based features. *Appl Soft Comput* 22:94–100
106. Li Q, Feng B, Xie L, Liang P, Zhang H, Wang T (2016) A cross-modality learning approach for vessel segmentation in retinal images. *IEEE Trans Med Imaging* 35(1):109–118
107. Sironi A, Tekin B, Rigamonti R, Lepetit V, Fua P (2015) Learning separable filters. *IEEE Trans Pattern Anal Mach Intell* 37(1):94–106
108. Ceylan M, Yasar H (2016) A novel approach for automatic blood vessel extraction in retinal images: complex ripplelet-I transform and complex valued artificial neural network. *Turk J Electr Eng Comput Sci* 24(4):3212–3227
109. Liskowski P, Krawiec K (2016) Segmenting retinal blood vessels with deep neural networks. *IEEE Trans Med Imaging* 35(11):2369–2380
110. Fraz M, Remagnino P, Hoppe A, Uyyanonvara B, Rudnicka A, Owen C, Barman S (2012) Ensemble classification system applied for retinal vessel segmentation on child images containing various vessel profiles. In: *Image analysis and recognition*. Springer, Berlin Heidelberg, pp 380–389
111. Fraz M, Remagnino P, Hoppe A, Uyyanonvara B, Rudnicka A, Owen C, Barman S (2012) An ensemble classification-based approach applied to retinal blood vessel segmentation. *IEEE Trans Biomed Eng* 59(9):2538–2548
112. Fraz M, Rudnicka A, Owen C, Barman S (2014) Delineation of blood vessels in pediatric retinal images using decision trees-based ensemble classification. *Int J Comput Assist Radiol Surg* 9(5):795–811
113. Wang S, Yin Y, Cao G, Wei B, Zheng Y, Yang G (2015) Hierarchical retinal blood vessel segmentation based on feature and ensemble learning. *Neurocomputing* 149:708–717
114. Welikala R, Fraz M, Foster P, Whincup P, Rudnicka A, Owen C, Strachan D, Barman S (2016) Automated retinal image quality assessment on the UK Biobank dataset for epidemiological studies. *Comput Biol Med* 71:67–76
115. Zhu C, Zou B, Xiang Y, Cui J, Wu H (2016) An ensemble retinal vessel segmentation based on supervised learning in fundus images. *Chin J Electron* 25(3):503–511

116. Liu I, Sun Y (1993) Recursive tracking of vascular networks in angiograms based on the detection-deletion scheme. *IEEE Trans Med Imaging* 12:334–341
117. Chutatape O, Liu Z, Krishnan SM (1998) Retinal blood vessel detection and tracking by matched Gaussian and Kalman filters. In: *Engineering in medicine and biology society, 1998. Proceedings of the 20th annual international conference of the IEEE*, vol 20, no 6, pp 3144–3149
118. Toliás Y, Panas S (1998) A fuzzy vessel tracking algorithm for retinal images based on fuzzy clustering. *IEEE Trans Med Imaging* 17(2):263–273
119. Can A, Shen H, Turner J, Tanenbaum H, Roysam B (1999) Rapid automated tracing and feature extraction from retinal fundus images using direct exploratory algorithms. *IEEE Trans Inf Technol Biomed* 3(2):125–138
120. Lalonde M, Gagnon L, Boucher M (2000) Non-recursive paired tracking for vessel extraction from retinal images. In: *Vision interface*, pp 61–68
121. Quek F, Kirbas C (2001) Vessel extraction in medical images by wave-propagation and traceback. *IEEE Trans Med Imaging* 20(2):117–131
122. Delibasis K, Kechriniotis A, Tsonos C, Assimakis N (2010) Automatic model-based tracing algorithm for vessel segmentation and diameter estimation. *Comput Methods Programs Biomed* 100(2):108–122
123. Xu X, Niemeijer M, Song Q, Sonka M, Garvin M, Reinhardt J, Abramoff M (2011) Vessel boundary delineation on fundus images using graph-based approach. *IEEE Trans Med Imaging* 30(6):1184–1191
124. Huang Y, Zhang J, Huang Y (2012) An automated computational framework for retinal vascular network labeling and branching order analysis. *Microvasc Res* 84(2):169–177
125. Yin Y, Adel M, Bourennane S (2012) Retinal vessel segmentation using a probabilistic tracking method. *Pattern Recognit* 45(4):1235–1244
126. Nayeibifar B, Moghaddam H (2013) A novel method for retinal vessel tracking using particle filters. *Comput Biol Med* 43(5):541–548
127. Fraz M, Remagnino P, Hoppe A, Rudnicka A, Owen C, Whincup P, Barman S (2013) Quantification of blood vessel calibre in retinal images of multi-ethnic school children using a model based approach. *Comput Med Imaging Graph* 37(1):48–60
128. Yin Y, Adel M, Bourennane S (2013) Automatic segmentation and measurement of vasculature in retinal fundus images using probabilistic formulation. *Computational and mathematical methods in medicine 2013*:260410–260410
129. Vázquez S, Cancela B, Barreira N, Penedo M, Rodríguez-Blanco M, Seijo M, Tuero GD, Barceló M, Saez M (2013) Improving retinal artery and vein classification by means of a minimal path approach. *Mach Vis Appl* 24(5):919–930
130. Bekkers E, Duits R, Berendschot T, Romeny BTH (2014) A multi-orientation analysis approach to retinal vessel tracking. *J Math Imaging Vis* 49(3):583–610
131. De J, Ma T, Li H, Dash M, Li C (2013) Automated tracing of retinal blood vessels using graphical models. In: *Image analysis*. Springer, Berlin, pp 277–289
132. De J, Li H, Cheng L (2014) Tracing retinal vessel trees by transductive inference. *BMC Bioinform* 15(1):20
133. Poletti E, Ruggeri A (2014) Graph search retinal vessel tracking. In: *Ophthalmological imaging and applications*, pp 97–115
134. Zhang J, Li H, Nie Q, Cheng L (2014) A retinal vessel boundary tracking method based on Bayesian theory and multi-scale line detection. *Comput Med Imaging Graph* 38(6):517–525
135. Cheng L, De J, Zhang X, Lin F, Li H (2014) Tracing retinal blood vessels by matrix-forest theorem of directed graphs. In: *Medical image computing and computer-assisted intervention—MICCAI*, Springer, pp 626–633
136. Chen D, Cohen L (2015) Piecewise geodesics for vessel centerline extraction and boundary delineation with application to retina segmentation. In: *Scale space and variational methods in computer vision*, pp 270–281
137. Vermeer K, Vos F, Lemij H, Vossepoel A (2004) A model based method for retinal blood vessel detection. *Comput Biol Med* 34(3):209–219
138. Huber P (1965) A robust version of the probability ratio test. *Ann Math Stat* 36(6):1753–1758
139. Field C, Smith B (1994) Robust estimation: a weighted maximum likelihood approach. *Int Stat Rev* 405–424
140. Ronchetti E (1985) Robust model selection in regression. *Stat Probab Lett* 3(3):21–23
141. Mahadevan V, Narasimha-Iyer H, Roysam B, Tanenbaum H (2004) Robust model-based vasculature detection in noisy biomedical images. *IEEE Trans Inf Technol Biomed* 8(3):360–376
142. Narasimha-Iyer H, Mahadevan V, Beach J, Roysam B (2008) Improved detection of the central reflex in retinal vessels using a generalized dual-Gaussian model and robust hypothesis testing. *IEEE Trans Inf Technol Biomed* 12(3):406–410
143. Alonso-Montes C, Vilarino D, Penedo M (2005) On the automatic 2D retinal vessel extraction. In: *Pattern recognition and image analysis*. Springer, Berlin, pp 165–173
144. Perfetti R, Ricci E, Casali D, Costantini G (2007) Cellular neural networks with virtual template expansion for retinal vessel segmentation. *IEEE Trans Circuits Syst II Express Briefs* 54(2):141–145
145. Wang L, Bhalerao A, Wilson R (2007) Analysis of retinal vasculature using a multi-resolution hermite model. *IEEE Trans Med Imaging* 26(2):137–152
146. Narasimha-Iyer H, Beach J, Khoobehi B, Roysam B (2007) Automatic identification of retinal arteries and veins from dual-wavelength images using structural and functional features. *IEEE Trans Biomed Eng* 54(8):1427–1435
147. Lam B, Yan H (2008) A novel vessel segmentation algorithm for pathological retina images based on the divergence of vector fields. *IEEE Trans Med Imaging* 27(2):237–246
148. Alonso-Montes C, Vilarino D, Dudek P, Penedo M (2008) Fast retinal vessel tree extraction: a pixel parallel approach. *Int J Circuit Theory Appl* 36(5–6):641–651
149. Alonso-Montes C, Vilarino D, Penedo M (2005) CNN-based automatic retinal vascular tree extraction. In: *Cellular neural networks and their applications, 2005 9th International Workshop*. IEEE, pp 61–64
150. Dudek P, Carey S (2006) General-purpose 128/spl times/128 SIMD processor array with integrated image sensor. *Electron Lett* 42(12):678–679
151. Vilarino D, Rekeczky C (2004) Implementation of a pixel-level snake algorithm on a CNUM-based chip set architecture. *IEEE Trans Circuits Syst I Regul Pap* 51(5):885–891
152. Lam B, Gao Y, Liew A (2010) General retinal vessel segmentation using regularization-based multiconcavity modeling. *IEEE Trans Med Imaging* 29(7):1369–1381
153. Gao X, Bharath A, Stanton A, Hughes A, Chapman N, Thom S (2001) A method of vessel tracking for vessel diameter measurement on retinal images. In: *Image processing, proceedings 2001 international conference*. IEEE, vol 2, pp 881–884
154. Zhu T (2010) Fourier cross-sectional profile for vessel detection on retinal images. *Comput Med Imaging Graph* 34(3):203–212
155. Kovsi P (2003) Phase congruency detects corners and edges. In: *The Australian pattern recognition society conference: DICTA*
156. Kovács G, Hajdu A (2016) A self-calibrating approach for the segmentation of retinal vessels by template matching and contour reconstruction. *Med Image Anal* 29:24–46

157. Kass M, Witkin A, Terzopoulos D (1988) Snakes: active contour models. *Int J Comput Vis* 1(4):321–331
158. McInerney T, Terzopoulos D (2000) T-snakes: topology adaptive snakes. *Med Image Anal* 4(2):73–91
159. McInerney T, Hamarneh G, Shenton M, Terzopoulos D (2002) Deformable organisms for automatic medical image analysis. *Med Image Anal* 6(3):251–266
160. Nain D, Yezzi A, Turk G (2004) Vessel segmentation using a shape driven flow. In: *Medical image computing and computer-assisted intervention—MICCAI*. Springer, Berlin, pp 51–59
161. Espona L, Carreira M, Ortega M, Penedo M (2007) A snake for retinal vessel segmentation. In: *Pattern recognition and image analysis*. Springer, Berlin, pp 178–185
162. Al-Diri B, Hunter A, Steel D (2009) An active contour model for segmenting and measuring retinal vessels. *IEEE Trans Med Imaging* 28(9):1488–1497
163. Chan T, Vese L (2001) Active contours without edges. *IEEE Trans Image Process* 10(2):266–277
164. Sum K, Cheung P (2008) Vessel extraction under non-uniform illumination: a level set approach. *IEEE Trans Biomed Eng* 55(1):358–360
165. Zhang Y, Hsu W, Lee M (2009) Detection of retinal blood vessels based on nonlinear projections. *J Signal Process Syst* 55(1–3):103–112
166. Oloumi F, Rangayyan R, Ells A (2012) Parabolic modeling of the major temporal arcade in retinal fundus images. *IEEE Trans Instrum Meas* 61(7):1825–1838
167. Rouchdy Y, Cohen L (2013) Geodesic voting methods: overview, extensions and application to blood vessel segmentation. *Comput Methods Biomech Biomed Eng Imaging Vis* 1(2):79–88
168. Guo Z, Lin P, Ji G, Wang Y (2014) Retinal vessel segmentation using a finite element based binary level set method. *Inverse Probl Imaging* 8(2):459–473
169. Lermé N, Rossant F, Bloch I, Paques M, Koch E (2014) Coupled parallel snakes for segmenting healthy and pathological retinal arteries in adaptive optics images. In: *Image analysis and recognition*. Springer, pp 311–320
170. Zhao Y, Rada L, Chen K, Harding S (2015) Automated vessel segmentation using infinite perimeter active contour model with hybrid region information with application to retinal images. *IEEE Trans Med Imaging* 34(9):1797–1807
171. Wang L, Zhang H, He K, Chang Y, Yang X (2015) Active contours driven by multi-feature gaussian distribution fitting energy with application to vessel segmentation. *PLoS ONE* 10(11):e0143105
172. Rad AE, Rahim MSM, Kolivand H, Amin IBM (2017) Morphological region-based initial contour algorithm for level set methods in image segmentation. *Multimed Tools Appl* 76(2):2185–2201
173. Oliveira W, Teixeira J, Ren T, Cavalcanti G, Sijbers J (2016) Unsupervised retinal vessel segmentation using combined filters. *PLoS ONE* 11(2):e0149943
174. Nieto A, Brea V, Vilariño D (2009) FPGA-accelerated retinal vessel-tree extraction. In: *Field programmable logic and applications, FPL 2009*. International conference, IEEE, pp 485–488
175. Krause M, Alles RM, Burgeth B, Weickert J (2016) Fast retinal vessel analysis. *J Real Time Image Process* 11(2):413–422
176. Koukounis D, Ttofis C, Papadopoulos A, Theocharides T (2014) A high performance hardware architecture for portable, low-power retinal vessel segmentation. *Integr VLSI J* 47(3):377–386
177. Argüello F, Vilariño DL, Heras DB, Nieto A (2018) GPU-based segmentation of retinal blood vessels. *J Real Time Image Process* 14(4):773–782
178. Villalobos-Castaldi F, Felipe-Riverón E, Sánchez-Fernández L (2010) A fast, efficient and automated method to extract vessels from fundus images. *J Vis* 13(3):263–270
179. Condurache A, Mertins A (2012) Segmentation of retinal vessels with a hysteresis binary-classification paradigm. *Comput Med Imaging Graph* 36(4):325–335
180. Mudassar A A, Butt S (2013) Extraction of blood vessels in retinal images using four different techniques. *J Med Eng* 2013:408120–408120
181. Salazar-Gonzalez A, Kaba D, Li Y, Liu X (2014) Segmentation of blood vessels and optic disc in retinal images. *IEEE J Biomed Health Inf* 18(6):1874–1886
182. Jiang K, Zhou Z, Geng X, Zhang X, Tang L, Wu H, Dong J (2015) Isotropic undecimated wavelet transform fuzzy algorithm for retinal blood vessel segmentation. *J Med Imaging Health Inf* 5(7):1524–1527
183. Dai P, Luo H, Sheng H, Zhao Y, Li L, Wu J, Zhao Y, Suzuki K (2015) A new approach to segment both main and peripheral retinal vessels based on gray-voting and gaussian mixture model. *PLoS ONE* 10(6):e0127748
184. Fumero F, Alayón S, Sanchez J, Sigut J, Gonzalez-Hernandez M (2011) RIM-ONE: an open retinal image database for optic nerve evaluation. In: *Computer-based medical systems (CBMS), 2011 24th international symposium, IEEE*, pp 1–6
185. Niemeijer M, Staal J, Ginneken B, Loog M, Abramoff M (2004) DRIVE: digital retinal images for vessel extraction. <http://www.isi.uu.nl/Research/Databases/DRIVE>
186. MESSIDOR: Methods for evaluating segmentation and indexing techniques dedicated to retinal ophthalmology (2004) <http://messidor.crihan.fr/index-en.php>
187. ARIA online, retinal image archive (2006) http://www.eyecharity.com/aria_online.html
188. Kauppi T, Kalesnykiene V, Kamarainen JK, Lensu L, Sorri I, Raninen A, Voutilainen R, Uusitalo H, Kälviäinen H, Pietil J (2007) DIARETDB1 diabetic retinopathy database and evaluation protocol. *Proc Med Image Underst Anal MIUA* 1:3–7
189. IMAGERET-optimal detection and decision-support diagnosis of diabetic retinopathy. <http://www.it.lut.fi/project/imageret/>
190. Al-Diri B, Hunter A, Steel D, Habib M, Hudaid T, Berry S (2008) REVIEW-a reference data set for retinal vessel profiles. In: *Engineering in medicine and biology society. EMBS 2008, 30th annual international conference of the IEEE*, pp 2262–2265
191. Carmona E, Rincón M, García-Feijoo J, Martínez-de-la-Casa J (2008) Identification of the optic nerve head with genetic algorithms. *Artif Intell Med* 43(3):243–259
192. García-Feijoo J, Martínez-de-la-Casa JM, Carmona E, Rincón M, Mayoral M (2008) DRIONS-DB. <http://www.ia.uned.es/~ejcarmona/DRIONS-DB.html>
193. Niemeijer M, Ginneken BV, Cree M, Mizutani A, Quéllec G, Sánchez C, Zhang B, Hornero R, Lamard M, Muramatsu C, Wu X (2010) Retinopathy online challenge: automatic detection of microaneurysms in digital color fundus photographs. *IEEE Trans Med Imaging* 29(1):185–195
194. Budai A, Hornegger J, Michelson G (2009) Multiscale approach for blood vessel segmentation on retinal fundus images. *Invest Ophthalmol Vis Sci* 50(13):325
195. The VICAVR database (2010) <http://www.varpa.es/vicavr.html>
196. Giancardo L, Meriaudeau F, Karnowski T, Li Y, Garg S, Tobin K, Chaum E (2012) Exudate-based diabetic macular edema detection in fundus images using publicly available datasets. *Med Image Anal* 16(1):216–226
197. Prentas P, Loncaric S, Vatauvuk Z, Bencic G, Subasic M, Petkovic T, Dujmovic L, Malenica-Ravlic M, Budimlija N, Tadic R (2013) Diabetic retinopathy image database (DRiDB): a new database for diabetic retinopathy screening programs research. In: *Image and signal processing and analysis (ISPA), 2013 8th international symposium*, pp 711–716
198. Shahbeig S (2013) Automatic and quick blood vessels extraction algorithm in retinal images. *IET Image Proc* 7(4):392–400